



**DEPARTMENT OF INTERNATIONAL AND
EUROPEAN ECONOMIC STUDIES**

ATHENS UNIVERSITY OF ECONOMICS AND BUSINESS

**CLIMATE CHANGE IMPACT
ON ECONOMIC GROWTH:
REGIONAL CLIMATE POLICY UNDER
COOPERATION AND NONCOOPERATION**

YONGYANG CAI

WILLIAM BROCK

ANASTASIOS XEPAPADEAS

Working Paper Series

22-14

April 2022

Climate Change Impact on Economic Growth: Regional Climate Policy under Cooperation and Noncooperation *

Yongyang Cai[†] William Brock[‡] Anastasios Xepapadeas[§]

April 7, 2022

Abstract

We compute regional social cost of carbon (SCC) in the face of climate change impact on the rate of growth of regional GDP under cooperation and noncooperation between regions with climate feedbacks and heat transfer present or missing. Climate damage to economic growth poses serious challenges for many countries, particularly in the tropic region. We find that in the presence of climate damage to economic growth, regional SCC is high in either a cooperative world or a noncooperative world, implying that it is optimal for each region to choose stringent climate policies. Moreover, relatively to cooperation, noncooperation reduces GDP of countries in both the high northern latitudes and the tropic region while the loss for the developing countries in the tropic region is significant. Our results are robust with different modeling of the climate impact.

Keywords: Integrated Assessment Model of climate and economy, spatial heat transport, regional social cost of carbon, carbon tax, Nash equilibrium, economic growth, climate feedbacks

JEL Classification: Q54, Q58

1 Introduction

One major uncertainty in climate change economics is how much damage to an economy climate change will impose. DICE (Nordhaus, 2008, 2017b) uses a quadratic damage function

*Cai and Brock acknowledge support from the National Science Foundation grant SES-1463644.

[†]Department of Agricultural, Environmental and Development Economics, The Ohio State University. cai.619@osu.edu

[‡]Department of Economics, University of Wisconsin-Madison and University of Missouri-Columbia. wbrock@ssc.wisc.edu

[§]Department of International and European Economic Studies, Athens University of Economics and Business; Department of Economics, University of Bologna. xepapad@aueb.gr

so that the damage to instantaneous output will be 7.8% or 25.4% if global average atmospheric temperature increases 6°C or 12°C over the preindustrial level. Since DICE assumes a perfect foresight dynamic model using the quadratic damage function, it provides a relatively low social cost of carbon (SCC). Weitzman (2012) points out that this significantly underestimates the catastrophic climate damage. He then changes the quadratic damage function by adding a new term: a power function of temperature increase with the exponent 6.754. The coefficient of the additional term is very small so that it has almost no impact on damage when temperature increase is lower than 2°C, but it leads to 50% or 99% damage to output if temperature increase is 6°C or 12°C, and thus it implies a significantly higher SCC.¹

In addition to climate damage to instantaneous output, researchers also find that climate change can reduce economic growth.² Evidence indicates that there are large and negative effects of higher temperatures on growth in poor countries in low-latitude regions. Dell et al. (2012) find an $\sim 1.3\%$ reduction in economic growth for a 1°C increase in global temperature, while Moore and Diaz (2015) and Dietz and Stern (2015) find that climate damage to economic growth increases the global SCC significantly. Rezai et al. (2018) show that climate damage to economic growth leads to a dystopian income distribution if no climate policy is imposed. Diffenbaugh and Burke (2019) show that global warming increases economic inequality, as it reduces annual economic growth in hotter and poorer countries but it increases in many cooler and wealthier countries relative to a world without anthropogenic warming. However, they do not analyze regional scale issues under the richer and more detailed climate dynamics as we do here.³

Empirical findings in the literature are still ambiguous about whether global warming reduces instantaneous output or economic growth. For example, Dell et al. (2012) show that the effects of temperature persist for 10 to 15 years in poor countries. Burke et al. (2015b) and Burke et al. (2018) find that global warming impacts economic growth, leading to higher income in the high northern latitudes, but significant loss in the tropic region. Kalkuhl and Wenz (2020) find that temperature affects productivity levels considerably but there is no evidence of its impact on permanent growth rate if non-market impacts and costs due to sea-level rise are excluded. Kahn et al. (2021) argue that all regions (cold or hot, and rich or poor) will experience a relatively large fall in gross domestic product (GDP) per capita by 2100 if there are no climate policies.⁴

¹Dietz and Stern (2015) apply Weitzman’s (2012) damage function to show this.

²Economic growth in this paper means the growth of GDP.

³The literature also discusses the SCC under uncertainties of climate damage, see e.g. Cai et al. (2016), Cai et al. (2017), Cai and Lontzek (2019), Barnett et al. (2020), Dietz et al. (2021a), and the recent review article by Cai (2021).

⁴See Carleton and Hsiang (2016), Heal and Park (2016), Auffhammer (2018), Kolstad and Moore (2020),

Our model follows recent research work to assume that the temperature anomaly affects economic growth, by modeling it with climate impact on the growth rate of TFP (total factor productivity) or ten-year lagged climate impact on TFP levels. We calibrate climate impact using the projection GDP data of Burke et al. (2018). The model also incorporates heat transfer from low latitudes to high latitudes as well as climate feedbacks leading to polar amplification,⁵ which means that warming in the high latitudes increases faster than in the tropic region. Our results are in line with recent findings suggesting that damages from temperature increases at low latitudes are much higher than at high latitudes.⁶

Almost every Integrated Assessment Model (IAM) (e.g., DICE) uses a social planner’s model assuming that countries are unselfish and the social planner can allocate resources between countries without any border friction. But if we have multiple regions in a model, then this “unselfish region” assumption will lead to extremely large capital flows between regions (from rich regions to poor regions), as discussed in the pure Negishi solution in Nordhaus and Yang (1996). To avoid the unrealistic compensatory income wealth between regions, one way is to impose border frictions as in Cai et al. (2019). In this paper, for simplicity we use an alternative way that assumes that the regional economy is closed so there is no capital flow between regions (but for each region, the social planner can allocate resources between countries inside the region without any border friction). That is, the cooperation between regions in our social planner’s problem happens only on the mitigation (which will of course affect consumption and capital investment). But this is a polar solution of the extreme case.

In this paper, besides this social planner’s solution, we also provide an open-loop Nash equilibrium solution in the other extreme case when regions are noncooperative and maximize own utility taking into account climate change damages to own output. Climate policy under cooperation and noncooperation between regions has been studied in the literature. For example, Dutta and Radner (2009) have a theoretical analysis of a dynamic commons game for modeling the global warming process, in which the players are countries. RICE (Nordhaus, 2010) studies the regional SCC under a social planner’s model with weights on regional utilities, so it does not study noncooperative outcomes.⁷ Van der Ploeg and de Zeeuw

Neumann et al. (2020), and Cai (2021) for more discussion about the climate impact on output levels and growth rates.

⁵Stuecker et al. (2018) show that the main causes of polar amplification are the lapse-rate feedback, the Planck feedback and the surface-albedo feedback.

⁶See for example Meinshausen et al. (2011a), Burke et al. (2015b), Dennig et al. (2015), Hsiang et al. (2017), Burke et al. (2018), and Kalkuhl and Wenz (2020).

⁷However an earlier version of RICE (Nordhaus and Yang, 1996) does study non-cooperative equilibria and compares with the cooperative case. To our knowledge, none of the RICE type models has heat transport or climate damage to economic growth as does our model.

(2016) and Jaakkola and van der Ploeg (2019) study tipping points without geographical regional specification and poleward heat transport. Brock and Xepapadeas (2019) include heat transport and regional specification but they use a very simplified climate model without multi-layer modeling of the carbon cycle and focus on the Northern Hemisphere only. Moreover, van der Ploeg and de Zeeuw (2016), Jaakkola and van der Ploeg (2019), and Brock and Xepapadeas (2019) use continuous time models and solve the associated Hamilton-Jacobi-Bellman equations or Hamiltonian systems. Cai et al. (2019) build a dynamic stochastic IAM with two regions to solve the optimal regional carbon taxes under cooperation and feedback Nash equilibrium with heat transport, sea level rise, permafrost thawing, adaptation, and climate tipping risks. They find optimal regional carbon taxes in the high northern latitude region are higher than in the tropic region in both cooperative and noncooperative worlds.

However, none of these papers accounts for climate damages to the rate of growth of regional GDP. Moreover, our model includes a more realistic heat transport system and climate feedbacks. Our results show very different patterns of climate policy relative to the other papers mentioned. For example, we find that cooperation under damages to the rate of growth of regional GDP does not lead to converging carbon taxes for the regions as shown in van der Ploeg and de Zeeuw (2016). This is particularly because we calibrate our climate impacted TFP models with the recent empirical work, Burke et al. (2018), which shows strongly asymmetric damages from climate change in the regions: the tropic region suffers severe climate damages, while the northern high latitude region has a little damage only.

A major finding of this paper is that in the presence of climate damage to economic growth, regional SCC is high for either a cooperative world or a noncooperative world. In our baseline case, under cooperation the initial regional SCC is \$806/tCO₂ (per ton of carbon dioxide) for the northern high latitude region, or \$117/tCO₂ for the tropic region, while under noncooperation the numbers become \$49/tCO₂ and \$137/tCO₂ for the northern high latitude region and the tropic region respectively.⁸ These numbers tell us that under either cooperation or noncooperation it is always optimal for each region to choose stringent climate policies. Moreover, in the baseline case, it is optimal for each region to keep the global mean atmospheric temperature anomaly in this century below 1.5°C under cooperation, or below 2°C under noncooperation. These are robust in our other five major cases.

The second interesting finding of this paper is that the regional SCC for the developed countries in the high northern latitudes is higher than for the developing countries in the tropic region in a cooperative world, although climate change has little impact on the economic growth of many countries in the high northern latitudes in this century. This is because

⁸We use US dollars (\$) per ton of carbon dioxide as the unit of SCC in this paper. The SCC per ton of CO₂ equals 12/44 times the SCC per ton of carbon.

consumption in the developing countries in the tropic region has higher marginal utility than in the developed countries in the northern region such that the social planner uses differentiated carbon taxes to achieve some second-best redistribution, under our assumption that there is no direct transfer of physical consumption or investment goods between the regions.

However, we find that relative to cooperation, noncooperation causes a little extra loss of GDP in the developed countries in the high northern latitudes but leads to significant loss for the developing countries in the tropic region. In our baseline case, noncooperation causes an extra 3.1% loss of output (i.e., \$2,393 per capita) in the northern region in 2100, relative to cooperation. But noncooperation reduces output by an extra 20% (i.e., \$6,907 per capita) in the tropic in 2100. In such a noncooperative world, the northern region has a much smaller SCC, and at the same time, the regional SCC for the tropic has no significant difference between cooperation and noncooperation, and noncooperative SCC are higher than cooperative SCC in the tropic in some cases. This is because climate change causes little impact in the northern region but it causes severe damage in the tropic, and the resulting higher emissions in the northern region mean the poor tropic is induced to set carbon prices higher: the initially poor and hot countries are made even poorer by severe climate change, driven by the selfish policies of the north, in comparison to the cooperative solution.

The third interesting finding of this paper is that if we model the climate change effect on TFP growth, then it will significantly increase the SCC, in comparison with the ten-year lagged effect of climate change on TFP levels, even when we use the same GDP scenarios for calibrating the TFP models. This tells us that we should pay attention to the modeling method for climate change effect.

In addition, we also show that not accounting for heat transfer and climate feedbacks introduces serious underestimation in the regional SCC. We consider this as an issue of important policy implications, since polar amplification is a real phenomenon which is not introduced in the popular type of simple regional IAMs.

The paper is organized as follows. Section 2 describes our model while some details are described in the appendices. Section 3 discusses cooperation and noncooperation. Section 4 shows our numerical results, including the comparison of regional SCC between the regions, between two specifications of climate damage (damage to TFP growth vs damage to TFP levels), between three GDP projection scenarios, and between two specifications of the climate system (considering polar amplification vs ignoring polar amplification). Section 5 concludes.

2 Model Setup

There are two main ways to partition the globe into multiple regions in an IAM. One way is to follow political and legal jurisdictions, but it can only have a rough approximation of the regional climate systems. For example, the RICE model (Nordhaus, 2010) – the regional version of DICE (Nordhaus, 2017a) – treats the climate system by using the globally averaged measure of temperature and neglects heat and moisture transport and especially polar amplification. Hassler and Krusell (2012) extend Golosov et al. (2014) to multi-regions. While their work is elegant, as is that of Golosov et al. (2014), they do not deal with poleward heat transport, multi-layer carbon cycles, and separation of atmospheric and oceanic layers, as we do here. Another way to partition the globe is to follow physical laws in modeling the regional climate systems (i.e., heat and moisture transfer between regions), but the regions may not have strong political and legal jurisdictions. For example, Langen and Alexeev (2007) build an IAM with two regions: the region from latitude 30°N to 90°N, and the region from latitude 0°N to 30°N.

In this study we define three regions over the globe for the temperature system: the North is the region north of latitude 30°N to 90°N (indexed as region 1), and the Tropic is the region from latitude 30°S to 30°N (indexed as region 2),⁹ and the South is the region from latitude 90°S (the south pole) to 30°S (indexed as region 3). The directionalities of heat and moisture transport are towards the North and the South from the Tropic (see Wunsch (2005, Figure 1)). For the economic system, since the South has relatively small amount of economic activity, we merge it with the Tropic, named with the Tropic/South (also indexed as region 2 for economic variables only for convenience). That is, we have two economic regions while our climate system has three regions. The disaggregation in these regions not only keeps track of the significant difference of their temperature systems, but also makes clear their significant economic difference since most countries in the Tropic/South are poor and more vulnerable to climate change and most countries in the North are rich and less vulnerable. Details of our model and methods are in the appendix. The structure of our model is depicted in Figure 1.

The economic module is based on a two-region differentiation of DICE-2016 (Nordhaus, 2017a). Krusell and Smith (2017) compare the two market structures of complete autarky and full international borrowing and lending and find that the market structures do not have a large impact on their results. We have ignored serious modeling of market structure in order to focus on some elements of geophysics that are ignored in other contributions,

⁹Our tropic region is a bit wider than the standard definition of the tropics in geography, i.e. [23.5°S, 23.5°N], in order to balance with economic variables and to follow Langen and Alexeev (2007) for the heat transfer system.

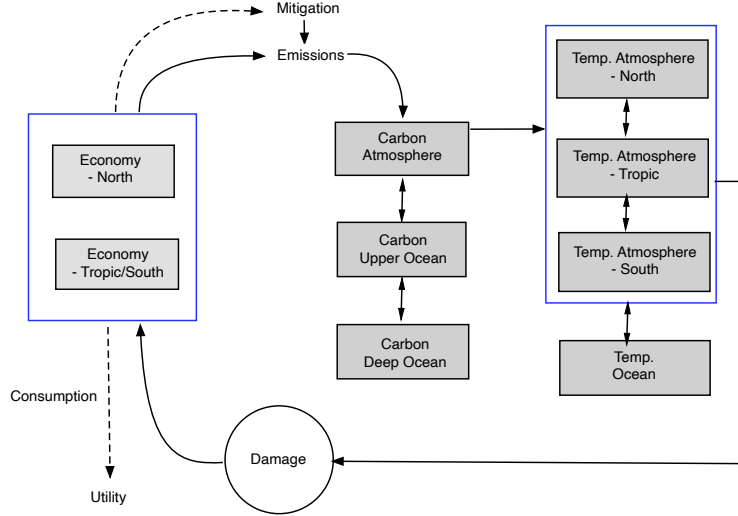


Figure 1: Schematic of our model. Under cooperation, the forward-looking social planner chooses mitigation and consumption in every economic region to maximize the sum of discounted regional utilities across economic regions over time. Regional warming impacts the economic growth in both the north and tropic/south regions. Under noncooperation, each economic region’s decision maker chooses their regional mitigation and consumption to maximize the sum of discounted utilities of their own region over time.

including that of Krusell and Smith (2017). We do this to provide new insights regarding the importance of spatial heat and moisture transport phenomena in climate change policy.

Desmet and Rossi-Hansberg (2015) and Desmet et al. (2021) suggest that labor mobility can dampen the costs of global warming. Here we assume labor mobility is exogenous and has already been addressed in the projection of populations in the economic regions. In our model we also ignore capital transfer between the economic regions for a more consistent comparison of solutions between cooperation and noncooperation, as noncooperation leads to no capital transfer (Cai et al., 2019). But inside each economic region there is no restriction on labor mobility or capital transfer as we assume countries inside one economic region are cooperative. We impose the constraint that there is no transfer of physical consumption or investment goods between the regions, in order to prevent the social planner from equalizing incomes between the two regions, as global income redistribution would distract from the main questions of mitigation of climate change.

2.1 Climate System

The climate system contains two modules: carbon cycle and temperature subsystem. Recently a “transient climate response to emissions” (TCRE) scheme has been employed for economic analysis (e.g., Brock and Xepapadeas, 2017; van der Ploeg, 2018; Dietz and Ven-

mans, 2019; Mattauch et al., 2020; Dietz et al., 2021b). The TCRE scheme assumes that contemporaneous globally or even regionally average atmospheric temperature increase is nearly linearly proportional to cumulative carbon emissions (Matthews et al., 2009; Leduc et al., 2016). However, Dietz et al. (2021b, Figure 5) show that the DICE-2016R’s (Nordhaus, 2017a) climate system does not lead to a large bias compared with the TCRE scheme using the welfare maximization criterion and the DICE-2016R’s economic system. More importantly, since our climate system follows the physical laws of the climate system to use DICE’s carbon cycle and our three-region temperature subsystem with heat transfer and climate feedbacks, it can be applied in future to study the impact of non-CO₂ radiative forcings, sea level rise, and solar engineering (a technology reflecting a small fraction of sunlight back into space or increasing the amount of solar radiation that escapes back into space to cool the planet).

We follow DICE-2016R (Nordhaus, 2017a) in using three layers of carbon concentrations: atmospheric carbon, carbon in the upper ocean, and carbon in the deep ocean. We denote them as $\mathbf{M}_t = (M_t^{\text{AT}}, M_t^{\text{UO}}, M_t^{\text{DO}})^\top$. The carbon cycle dynamics can be written as follows

$$\mathbf{M}_{t+1} = \Phi_{\mathbf{M}}\mathbf{M}_t + (E_t, 0, 0)^\top, \quad (1)$$

where E_t is the global carbon emission (billions of metric tons) and $\Phi_{\mathbf{M}}$ is the transition matrix calibrated against four RCP (Representative Concentration Pathways) scenarios, i.e., RCP2.6, RCP4.5, RCP6 and RCP8.5 (Meinshausen et al., 2011b). See Appendix A.1 for more details.

The global radiative forcing represents the CO₂ concentrations impact on the surface temperature of the globe (watts per square meter from 1900) and the non-CO₂ radiative forcing. We follow DICE-2016R to let the global radiative forcing be

$$F_t = \eta \log_2 (M_t^{\text{AT}}/M_*^{\text{AT}}) + F_t^{\text{EX}}, \quad (2)$$

where $\eta = 3.68$ and F_t^{EX} is the exogenous global non-CO₂ radiative forcing as in DICE-2016R.

We use $(T_{t,1}^{\text{AT}}, T_{t,2}^{\text{AT}}, T_{t,3}^{\text{AT}}, T_t^{\text{OC}})$ to represent the temperature anomaly (relative to 1900 levels) in the atmosphere (three regions) and the global ocean, where $T_{t,1}^{\text{AT}}, T_{t,2}^{\text{AT}}$ and $T_{t,3}^{\text{AT}}$ for

the North, the Tropic and the South respectively. Thus, the temperature system is

$$T_{t+1,1}^{\text{AT}} = (1 - \xi_5)T_{t,1}^{\text{AT}} - \xi_2 (T_{t,1}^{\text{AT}} - T_t^{\text{OC}}) + \xi_4 (T_{t,2}^{\text{AT}} - T_{t,1}^{\text{AT}}) + (\xi_1 + \xi_6)F_t, \quad (3)$$

$$\begin{aligned} T_{t+1,2}^{\text{AT}} &= (1 - \xi_5)T_{t,2}^{\text{AT}} - \xi_2 (T_{t,2}^{\text{AT}} - T_t^{\text{OC}}) - \frac{\xi_4}{2} (T_{t,2}^{\text{AT}} - T_{t,1}^{\text{AT}}) \\ &\quad - \frac{\xi_4}{2} (T_{t,2}^{\text{AT}} - T_{t,3}^{\text{AT}}) + (\xi_1 + \xi_7)F_t, \end{aligned} \quad (4)$$

$$T_{t+1,3}^{\text{AT}} = (1 - \xi_5)T_{t,3}^{\text{AT}} - \xi_2 (T_{t,3}^{\text{AT}} - T_t^{\text{OC}}) + \xi_4 (T_{t,2}^{\text{AT}} - T_{t,3}^{\text{AT}}) + \xi_1 F_t, \quad (5)$$

$$T_{t+1}^{\text{OC}} = T_t^{\text{OC}} + \xi_3 (T_{t,1}^{\text{AT}} - T_t^{\text{OC}}) + 2\xi_3 (T_{t,2}^{\text{AT}} - T_t^{\text{OC}}) + \xi_3 (T_{t,3}^{\text{AT}} - T_t^{\text{OC}}), \quad (6)$$

Here the parameter ξ_1 is the temperature increase for each unit of radiative forcing when there is no change in climate feedback, ξ_2 and ξ_3 represent additional heat transport between atmosphere and ocean due to temperature anomalies,¹⁰ ξ_4 is used to capture additional spatial heat and moisture transport between the North/South and the Tropic due to temperature anomalies, ξ_5 represents the sensitivity of the outgoing long-wave radiation to atmospheric temperature changes, ξ_6 and ξ_7 represent the aggregate effect of changes in climate feedbacks (e.g., the lapse-rate feedback, the Planck feedback, and the surface albedo feedback) below the preindustrial levels in the North and the South for each unit of radiative forcing (e.g., ice melting in the North reduces ice surface albedo feedback effect and then increases the amount of solar energy absorbed in the North’s atmosphere).¹¹ Since the area size of the Tropic is twice the one of the North or the South, the parameter ξ_4 is divided by 2 in the Tropic’s transition equation (4), and ξ_3 is multiplied by 2 for the difference of between the Tropic atmospheric temperature anomaly and the ocean temperature anomaly in the ocean’s transition equation (6). Moreover the global mean atmospheric temperature anomaly is $(T_{t,1}^{\text{AT}} + 2T_{t,2}^{\text{AT}} + T_{t,3}^{\text{AT}})/4$. We calibrate $\xi_1, \xi_2, \dots, \xi_7$ against the ensemble mean of CMIP5 (Navarro-Racines et al., 2020) models’ annual projections of temperature anomaly in every region under the four RCP scenarios until 2100. That is, we solve the following minimization problem:

$$\min_{\xi_1, \dots, \xi_7} \sum_{j=1}^4 \sum_{t=0}^{85} \left(\sum_{i=1}^3 \left| T_{t,i}^{\text{AT},j} - T_{t,i}^{\text{CMIP5,AT},j} \right| + \left| T_{t,i}^{\text{OC},j} - T_{t,i}^{\text{CMIP5,OC},j} \right| \right)$$

subject to the transition equations (3)-(6) for each RCP scenario $j = 1, \dots, 4$ (represented in the subscript) over the 85-year time horizon (from the initial year 2015 to 2100), and an

¹⁰Heat transport under no temperature anomalies has already been normalized to be zero, so for convenience we will just use “heat transport” or “heat transfer” to represent the additional heat transport due to temperature anomalies.

¹¹Since the South has little change in climate feedbacks in comparison with its preindustrial level, as its most area is ocean, we ignore it.

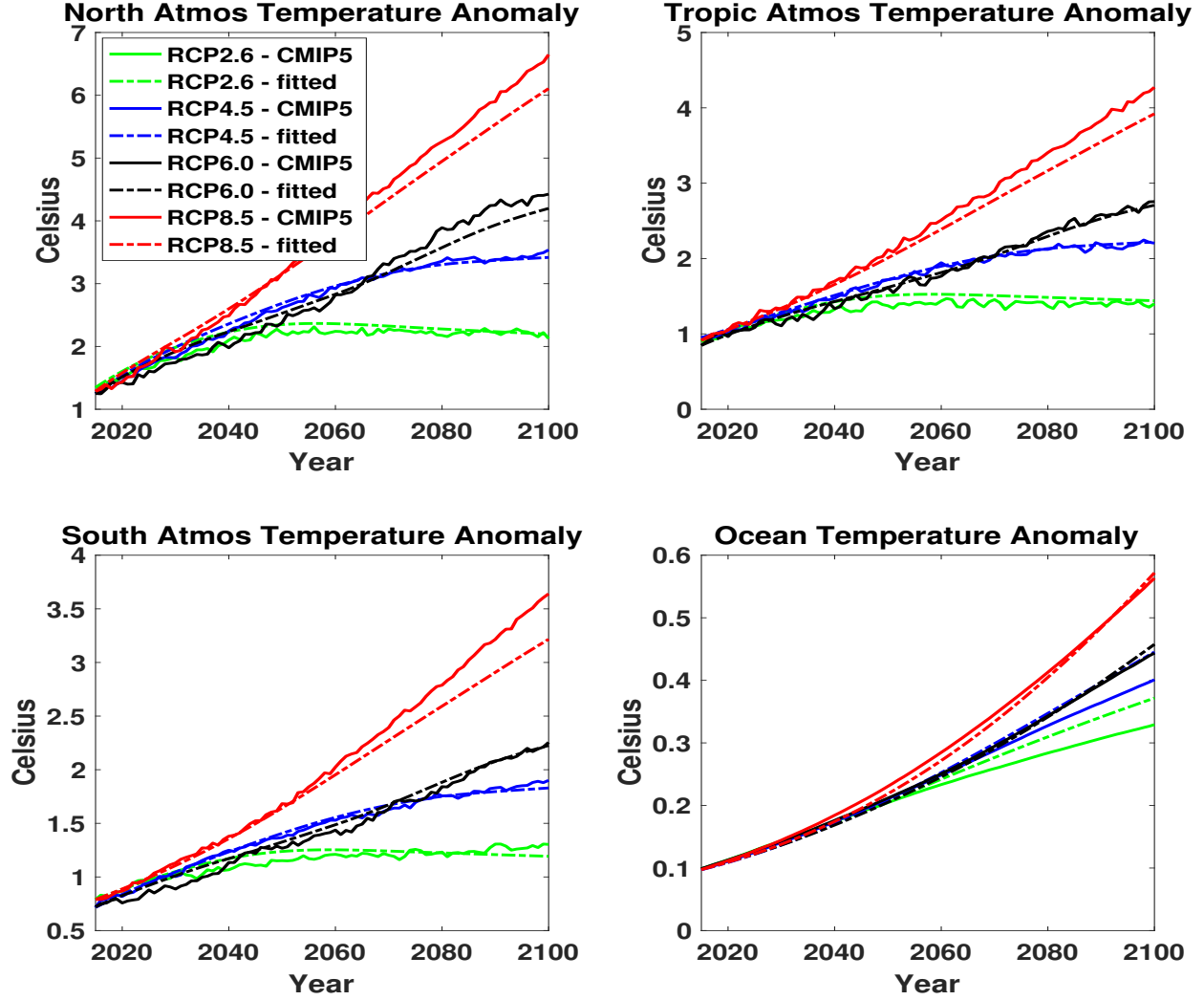


Figure 2: Fitting regional temperature anomaly under four RCP scenarios.

additional constraint $\xi_6 = (\xi_1 + (\xi_6 + 2\xi_7)/4) \eta / \xi_{\text{ECS}}$ such that our system's long-run global mean atmospheric temperature increase with a doubling of atmospheric carbon concentration is ξ_{ECS} , also known as the equilibrium climate sensitivity, which value is chosen to be 3.1 by following DICE-2016R.¹² Here the subscript ‘‘CMIP5’’ represents the data of the ensemble mean of CMIP5 models' annual projections, and the global radiative forcing F_t for each RCP scenario is given by Meinshausen et al. (2011b). Figure 2 shows that our fitted regional temperature anomaly in the North, the Tropic, the South, and the Ocean match well with the CMIP5 projections.

¹²For example, if we let $F_t = \eta$ (i.e., $M_t^{\text{AT}} = 2M_*^{\text{AT}}$ and $F_t^{\text{EX}} = 0$) since 2015, then our global mean temperature anomaly converges to 3.1°C after 5500 years under the transition equations (3)-(6) with our calibrated parameter values.

2.2 Economic System

Let $K_{t,i}$ be the regional capital state variables at time t and economic region $i = 1, 2$ (i.e., the North and the Tropic/South). Let $L_{t,i}$ be the exogenous regional population sizes. We follow DICE to let the regional gross output be

$$Y_{t,i} \equiv A_{t,i} K_{t,i}^\alpha L_{t,i}^{1-\alpha}, \quad (7)$$

where $\alpha = 0.3$, $A_{t,i}$ is regional total factor productivity (TFP) that will be affected by climate change, and we let the mitigation expenditure function be

$$\Psi_{t,i} \equiv \theta_{1,t,i} \mu_{t,i}^{\theta_2} Y_{t,i}$$

where $\mu_{t,i}$ are emission control rates, $\theta_2 = 2.8$, and $\theta_{1,t,i}$ are the exogenous abatement cost in fractions of output in economic region i at time t .

The global carbon emissions at time t are defined as

$$E_t \equiv \sum_{i=1}^2 E_{t,i}^{\text{Ind}} + E_t^{\text{Land}},$$

where E_t^{Land} is exogenous global carbon emissions from biological processes, and $E_{t,i}^{\text{Ind}} = \sigma_{t,i}(1 - \mu_{t,i})Y_{t,i}$ are industrial emissions, where $\sigma_{t,i}$ are the regional exogenous carbon intensity in region i .

The law of motion of the capital state variable $K_{t,i}$ is:

$$K_{t+1,i} = (1 - \delta_K)K_{t,i} + \widehat{Y}_{t,i} - c_{t,i}L_{t,i} \quad (8)$$

where $\delta_K = 0.1$ is the depreciation rate, $c_{t,i}$ is per capita consumption, and

$$\widehat{Y}_{t,i} \equiv Y_{t,i} - \Psi_{t,i} = (1 - \theta_{1,t,i} \mu_{t,i}^{\theta_2}) Y_{t,i}$$

is the net output.

2.3 Climate Impact to Economic Growth

Under the quadratic damage function of DICE for the Tropic, there is approximately 5% damage to output, if the tropic regional surface temperature increase is the same as the global mean surface temperature in 2100 under the RCP8.5 scenario, i.e., the temperature increase at 2100 is 4.7°C. However, this damage calculation ignores the climate impact on

regional economic growth shown in Burke et al. (2015b) and Burke et al. (2018), who show global nonlinear relationship between annual average temperature and growth rates in GDP per capita. Dell et al. (2012) show there are large and negative effects of higher temperatures on growth rates of per capita output for 10 to 15 years, but only in poor countries. Dell et al. (2012) use a linear function of temperature for the impact on growth rates of per capita output. Here we change it to be a quadratic function to reflect nonlinear effects as in Burke et al. (2015b) and Burke et al. (2018). Moyer et al. (2014) find that uncertainty in climate damage to economic growth creates a great range of estimates of the global SCC. Newell et al. (2021) show model uncertainty on growth effects is much larger than level effects. Barnett et al. (2021) argue that misspecification and ambiguity concerns loom larger under larger model uncertainty. In their framework the larger model uncertainty surrounding growth effects should lead to more prudent behavior than even large model uncertainty surrounding level effects since growth effects compound over time. Here we will deal with uncertainty in a rudimentary way by modeling growth effects or lagged level effects under different scenarios.

Burke et al. (2018) provide a baseline scenario of 165 countries' GDP paths, assuming temperature in year t changes the growth of GDP from year t to $t + 1$, under the RCP2.6 climate scenario and the SSP1 population scenario. They also provide a baseline scenario of the countries' GDP paths assuming one-year or five-year lagged temperature effect on GDP growth. In a dynamic model with endogenous GDP, the growth rate of GDP from year t to $t + 1$ may be impacted by the growth rate of regional TFP from t to $t + 1$, or the no-lagged or lagged impact of temperature anomaly on TFP levels as the climate damage to TFP levels will reduce output, then impact investment on next-period capital, then impact future GDP too. We first aggregate over Burke et al. (2018)' projected GDP of 165 countries to our two regional output for every year. In this study we will choose three GDP scenarios from 2015 to 2099 in each economic region for our calibration: the baseline scenario with contemporaneous temperature effect on GDP growth (called "GDP scenario 1"), the baseline scenario with one-year lagged temperature effect on GDP growth (called "GDP scenario 2"), and the baseline scenario with five-year lagged temperature effect on GDP growth (called "GDP scenario 3"). We will also choose two TFP model assumptions: ten-year lagged climate impact on regional TFP levels (called "TFP model 1"), and climate impact on regional TFP growth (called "TFP model 2").¹³

¹³We tried the TFP model assumption with the climate impact on regional TFP without lagged effect, and found that it cannot match well with any GDP data scenario, particularly for the Tropic/South. We also studied five-year lagged impact of temperature anomalies on regional TFP, and found that they are relatively less well fitted than ten-year lagged TFP model and that they do not have significant difference with the ten-year lagged impact. Thus we omit these analysis in this paper.

We first follow DICE to assume

$$A_{t+1,i}^{\text{EX}} = \frac{A_{t,i}^{\text{EX}}}{1 - g_{i,t}^{\text{TFP,EX}}}$$

is the exogenous regional TFP under no climate change for economic region $i = 1, 2$ (i.e., the North and the Tropic/South), where

$$g_{i,t}^{\text{TFP,EX}} = \zeta_{i,1}^{\text{TFP}} (1 - \exp(-\zeta_{i,2}^{\text{TFP}} t))$$

is the exogenous growth rate of regional TFP at time t under no climate impact. The initial TFP, $A_{0,i}^{\text{EX}}$, is chosen such that $Y_{0,i} = A_{0,i}^{\text{EX}} K_{0,i}^\alpha L_{0,i}^{1-\alpha}$ with the observed values of $Y_{0,i}$, $K_{0,i}$ and $L_{0,i}$ in the initial year 2015. Here $L_{t,i}$ are aggregated from Burke et al. (2018) under the Shared Socioeconomic Pathway 1 (SSP1) (Kc and Lutz, 2017; Riahi et al., 2017), which represents a world shifting toward a sustainable path taking the green road with low resource and energy intensity.¹⁴ We estimate $\zeta_{i,1}^{\text{TFP}}$ and $\zeta_{i,2}^{\text{TFP}}$ using the aggregated regional GDP from the 165 projected countries' GDP of Burke et al. (2018) under no climate impact. In our structural estimation of the parameters, for each pair of $(\zeta_{i,1}^{\text{TFP}}, \zeta_{i,2}^{\text{TFP}})$, we solve the following simple optimal growth model

$$\begin{aligned} \max_{c_{t,i}} \quad & \sum_{t=0}^{500} \beta^t u(c_{t,i}) L_{t,i}, \\ \text{s.t.} \quad & K_{t+1,i} = (1 - \delta_K) K_{t,i} + (y_{t,i} - c_{t,i}) L_{t,i}, \end{aligned} \quad (9)$$

for each economic region i , where $y_{t,i} = A_{t,i}^{\text{EX}} K_{t,i}^\alpha L_{t,i}^{1-\alpha}$ is the per-capita output affected by the parameters, β is the discount factor, and u is a per-capita utility function from consumption:

$$u(c) = \frac{c^{1-\gamma}}{1-\gamma} \quad (10)$$

where γ is elasticity of marginal utility. Here we follow DICE-2016R to choose $\gamma = 1.45$ and $\beta = 0.985$. We then use the solution of $y_{t,i}$ to compute its growth rates for matching the growth rates of the aggregated GDP of Burke et al. (2018) under no climate impact. That is, for each i , we find $(\zeta_{i,1}^{\text{TFP}}, \zeta_{i,2}^{\text{TFP}})$ such that

$$\sum_{t=0}^{83} \left(\frac{y_{t+1,i}}{y_{t,i}} - \frac{y_{t+1,i}^{\text{BDD,NoCC}}}{y_{t,i}^{\text{BDD,NoCC}}} \right)^2 \quad (11)$$

¹⁴Burke et al. (2018) provide 165 countries' population paths only in this century. We extend them until 2515 for our model, assuming no change after 2099.

is minimal, where $y_{t,i}$ and $y_{t,i}^{\text{BDD,NoCC}}$ are respectively the model (9)'s solution and the per-capita GDP of Burke et al. (2018) under no climate impact from 2015 to 2099. After we obtain the estimated values of $\zeta_{i,1}^{\text{TFP}}$ and $\zeta_{i,2}^{\text{TFP}}$ and their associated $g_{i,t}^{\text{TFP,EX}}$ and $A_{t,i}^{\text{EX}}$, we will use the GDP scenarios to estimate climate impact on TFP.

In our baseline case (i.e., case 1), we use the GDP scenario 1 to calibrate the TFP model 1, which assumes climate change has ten-year lagged effect on regional TFP levels, that is,

$$A_{t,i} = \frac{A_{t,i}^{\text{EX}}}{1 + \sum_{s=t-10}^t (\delta_i^{\text{TFP}})^{t-s} \left(\zeta_{i,3}^{\text{TFP}} (T_{s,i}^{\text{AT}} - T_{0,i}^{\text{AT}}) + \zeta_{i,4}^{\text{TFP}} (T_{s,i}^{\text{AT}} - T_{0,i}^{\text{AT}})^2 \right)} \quad (12)$$

where $T_{0,i}^{\text{AT}}$ is the temperature anomaly in our initial year (i.e., 2015), and the regional TFP in year t depends on year t' atmospheric temperature anomaly, $T_{t,i}^{\text{AT}}$, and last ten years'. The initial TFP $A_{0,i}$ is set to be $A_{0,i}^{\text{EX}}$. Here the regional atmospheric temperature anomalies $T_{s,i}^{\text{AT}}$ are the ensemble mean of CMIP5 models' annual projections under the RCP2.6 scenario used in Burke et al. (2018) for the GDP scenario 1. We use the GDP scenario 1 for calibrating parameters $(\zeta_{i,3}^{\text{TFP}}, \zeta_{i,4}^{\text{TFP}}, \delta_i^{\text{TFP}})$, where $\zeta_{i,3}^{\text{TFP}}$ and $\zeta_{i,4}^{\text{TFP}}$ represent the nonlinear climate impact of temperature increase on TFP levels, and δ_i^{TFP} represents the persistence factor of their impact at each economic region i . We apply the similar structural estimation method in finding $(\zeta_{i,1}^{\text{TFP}}, \zeta_{i,2}^{\text{TFP}})$ to estimate $(\zeta_{i,3}^{\text{TFP}}, \zeta_{i,4}^{\text{TFP}}, \delta_i^{\text{TFP}})$ under climate impact. That is, we let $y_{t,i} = A_{t,i} K_{t,i}^\alpha L_{t,i}^{-\alpha}$ using the TFP equation (12) with the pre-specified $A_{t,i}^{\text{EX}}$, and solve (9) repeatedly with different values of $(\zeta_{i,3}^{\text{TFP}}, \zeta_{i,4}^{\text{TFP}}, \delta_i^{\text{TFP}})$ until the distance between the growth rates of per capita GDP from (9) and the ones from the GDP scenario 1 is minimal.

In our case 2, we use the GDP scenario 1 to calibrate the TFP model 2, which assumes the growth of regional TFP from year t to $t+1$ depends on year t' atmospheric temperature anomaly. That is, we specify the paths of regional TFP at economic region i to be

$$A_{t+1,i} = \frac{A_{t,i}}{1 - g_{i,t}^{\text{TFP,EX}} \exp \left(- \left(\zeta_{i,3}^{\text{TFP}} (T_{t,i}^{\text{AT}} - T_{0,i}^{\text{AT}}) + \zeta_{i,4}^{\text{TFP}} (T_{t,i}^{\text{AT}} - T_{0,i}^{\text{AT}})^2 \right) \right)} \quad (13)$$

With this TFP model assumption, we estimate $(\zeta_{i,3}^{\text{TFP}}, \zeta_{i,4}^{\text{TFP}})$ to minimize the distance of growth rates of per capita output between the GDP scenario 1 and our model (9)'s solution with $y_{t,i} = A_{t,i} K_{t,i}^\alpha L_{t,i}^{-\alpha}$ using the TFP equation (13) and the pre-specified $g_{i,t}^{\text{TFP,EX}}$.

Figure 3 shows that our calibrated regional per capita outputs match well with the GDP scenario 1.¹⁵ Moreover, we see that climate change has little impact in the North

¹⁵The per-capita outputs of Burke et al. (2018) in Figure 3 are adjusted to start with our initial per capita output from the World Bank data of output in 2015, which are used for computing our initial TFP, but the growth rates are not adjusted. Note that we use the growth rates of Burke et al. (2018) for our calibration, so the calibrated parameter values of $\zeta_{i,1}^{\text{TFP}}, \dots, \zeta_{i,4}^{\text{TFP}}$ and δ_i^{TFP} are not affected by the adjustment.

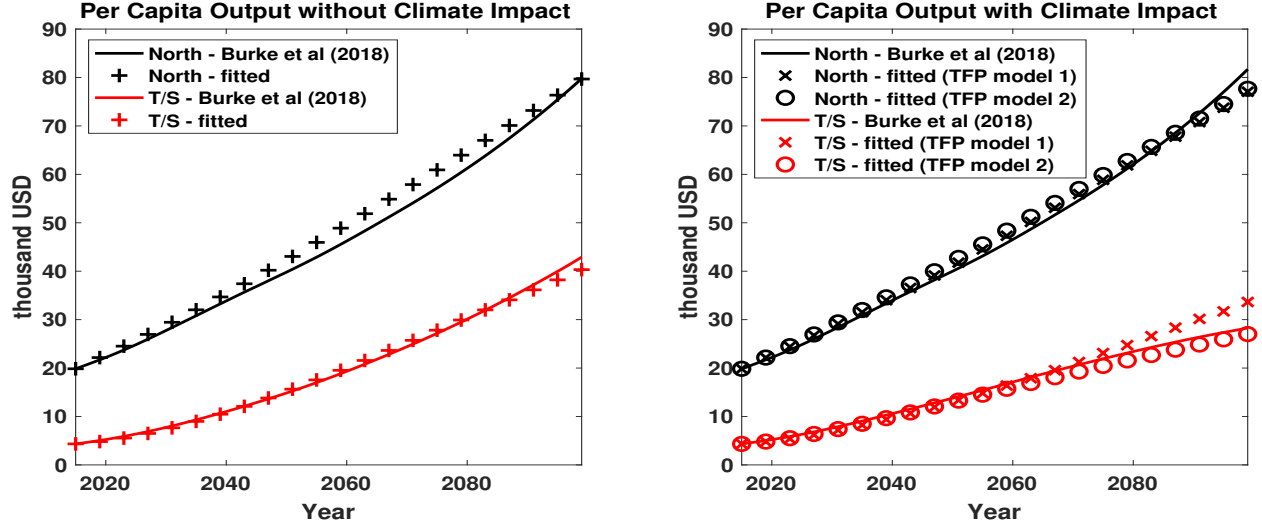


Figure 3: Fitting regional GDP with/without climate impact on economic growth in the baseline case (i.e., the TFP model 1 (12) calibrated with the GDP scenario 1). Left panel: regional per capita output without climate impact on economic growth; Right panel: regional per capita output with climate impact on economic growth. Black color: the North; Red color: the Tropic/South (i.e. T/S in the legend). Solid lines: per capita output from Burke et al. (2018); Marks: fitted per capita output of the North using the TFP model 1; Circles: fitted per capita output using the TFP model 2.

under the RCP2.6 climate scenario which controls the globally average temperature anomaly under around 1.5°C , but climate change significantly decreases per capita output in the Tropic/South from $\$42,905$ in 2099 to only $\$28,269$, i.e., 66% of its regional per capita output in a world without climate damage, under the GDP scenario 1. We caution that there is a substantial amount of uncertainty present in this kind of extrapolation. For example, Figure 3 may not account for all the uncertainties in adaptive responses in the Tropic/South to climate change, e.g. the Tropic/South may have a large increase of air conditioning, which may have large impact on economic production (Barreca et al., 2016).

In our cases 3-4 and 5-6, we use the GDP scenarios 2 and 3 respectively to calibrate the TFP models 1-2. Figure 4 shows that either of our TFP models 1-2 can lead to a good match with either of the GDP scenarios 2-3. The cases 3-4 associated with the GDP scenario 2 (the left panel of Figure 4) have a similar pattern with the baseline case: climate change has little impact in the North and substantial damage in the Tropic/South, but the damage is relatively less: climate change reduces the Tropic/South’s per capita output in 2099 to $\$33,567$, i.e., 78% of its per capita output in a world without climate damage, under the GDP scenario 2. However, in the cases 5-6 associated with the GDP scenario 3 (the right panel of Figure 4), climate change significantly reduces output in both economic regions: in 2099 the North has only $\$61,074$ (i.e., 77% of its regional per capita output in a world without climate

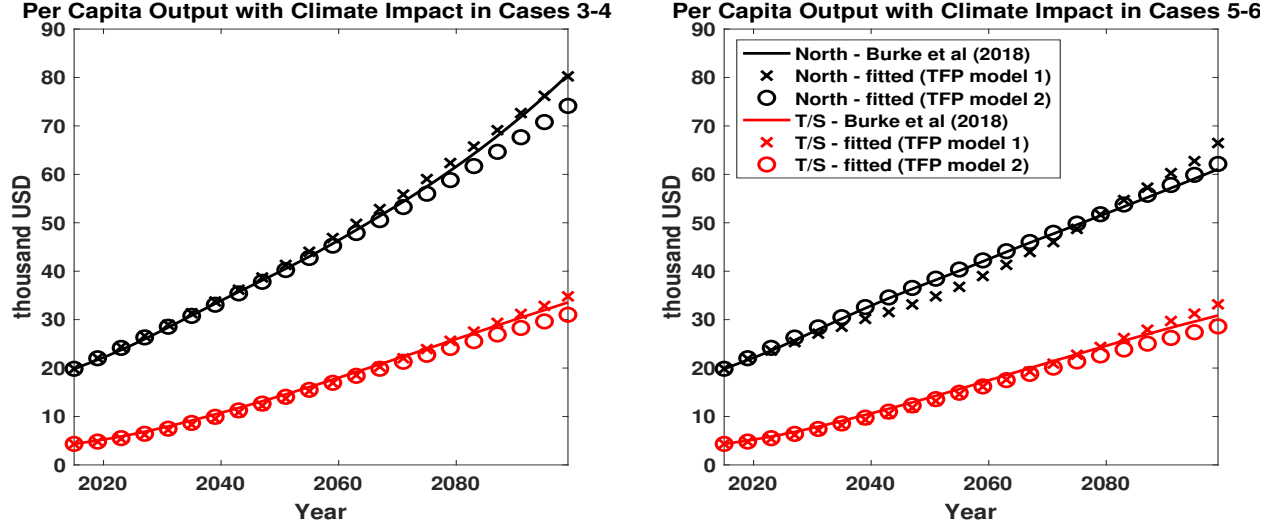


Figure 4: Fitting regional GDP with climate impact on economic growth under cases 3-4 and 5-6. Left panel: cases 3-4 (i.e., the TFP models 1-2 calibrated with the GDP scenario 2); Right panel: cases 5-6 (i.e., the TFP models 1-2 calibrated with the GDP scenario 3).

damage) and the Tropic/South has only \$30,865 (but is still higher than the GDP scenario 1). From the cases, we see that it has a huge uncertainty in the climate change impact in the North, while climate change always causes severe damages in the Tropic/South.

3 Cooperation and Noncooperation

We solve two dynamic models, one for a cooperative world, another for a noncooperative world.

3.1 Cooperative World

In our model under cooperation, a social planner maximizes the present value of the sum of regional utility across economic regions and time with annual time steps by choosing paths of per capita consumption and emission control rates. Our regional utility is equal to the product of regional population and per-capita utility, so the social welfare in each economic region i is

$$\sum_{t=0}^{\infty} \beta^t u(c_{t,i}) L_{t,i}.$$

The social planner solves the following dynamic optimization problem:

$$\max_{c_{t,i}, \mu_{t,i}} \sum_{t=0}^{\infty} \beta^t \sum_{i=1}^2 u(c_{t,i}) L_{t,i} \quad (14)$$

with four control variables $(c_{t,1}, c_{t,2}, \mu_{t,1}, \mu_{t,2})$ at each time t . The optimization is subject to the transition laws of three carbon concentration levels, four temperature levels, and two regional capital state variables. Since the choice of discount factor $\beta = 0.985$ makes the welfare after 500 years have little impact on the first 100 years' solutions, we follow DICE-2016R to approximate the infinite-horizon problem (14) by a finite-horizon problem with 500 years.

3.2 Noncooperative World

In our model under noncooperation, each economic region's decision maker maximizes the present value of the sum of their own regional utility across time by choosing their own paths of per capita consumption and emission control rates. That is, we simultaneously solve the following system of two dynamic optimization problems:

$$\max_{c_{t,i}, \mu_{t,i}} \sum_{t=0}^{\infty} \beta^t u(c_{t,i}) L_{t,i}, \quad i = 1, 2, \quad (15)$$

while each economic region's optimization is subject to the transition laws of three carbon concentration levels, four temperature levels, and their own regional capital, assuming that the other economic region's emission path is given. This is a dynamic game problem. We solve its open-loop Nash equilibrium (OLNE), that is, the optimal solution depends on only the initial condition and time. The concept of the OLNE could be interpreted as a situation in which individual agents, regions in our case, enter an agreement to commit to a future path of carbon emission at the beginning of the agreement. This type of equilibrium concept might not be as satisfactory - in terms of strong time consistency - as the feedback Nash equilibrium concept, but it has the computational advantages of solving open loop versus feedback,¹⁶ while the OLNE solution may be fairly close to the feedback Nash equilibrium.

¹⁶Solving feedback Nash equilibrium requires extensive supercomputer computing resources which are unavailable to the authors, as our model has 500 periods and 29 endogenous state variables (3 for carbon concentration levels, 4 for contemporaneous temperature levels in the regional atmosphere and ocean, 2 for regional capitals, and 20 for the 10 years' lagged atmospheric temperature anomalies in both economic regions), and value functions have kinks due to the occasionally binding constraint on the upper bound of emission control rates.

We use an iterative method to solve the OLNE, see Appendix A.2.

3.3 Regional Social Cost of Carbon and Carbon Tax

In Nordhaus (2017a), the regional SCC is defined to be the present value of future damages in a region caused by one extra ton of global carbon emissions in the current period. Ricke et al. (2018) use the same concept in computing country-level SCC (i.e. country-level contributions to the global SCC). But with their concept, we cannot derive that the optimal regional carbon tax is equal to the regional SCC, as the global SCC is the sum of their regional SCCs over all regions but the global carbon tax cannot be the sum of regional carbon taxes.

In this study, we follow van der Ploeg and de Zeeuw (2016) and Cai et al. (2019) to use a different concept of regional SCC, such that the regional SCC is equal to regional carbon tax when the emission control rate does not hit its lower or upper bound (Cai et al., 2017; Cai and Lontzek, 2019), where the regional carbon tax is defined as $-1000\theta_{1,t,i}\theta_{2,t,i}^{\theta_2-1}/\sigma_{t,i}$, following DICE, Cai et al. (2017) and Cai and Lontzek (2019). Thus, the regional SCC can be negative if the emission control rate hits its lower bound 0, or can be much larger than the regional carbon tax if the emission control rate hits its upper bound.

We define the regional cooperative SCC in economic region i as

$$\tau_{t,i}^{\text{SP}} = -1000 \left(\frac{\partial V_t^{\text{SP}}}{\partial M_t^{\text{AT}}} \right) / \left(\frac{\partial V_t^{\text{SP}}}{\partial K_{t,i}} \right)$$

where $V_t^{\text{SP}} = \max_{c_{s,i}, \mu_{s,i}} \sum_{s=t}^{\infty} \beta^t \sum_{i=1}^2 u(c_{s,i})L_{s,i}$ is the optimal global welfare starting from year t with a given starting state vector $(K_{t,1}, K_{t,2}, M_t^{\text{AT}}, \dots)$. In its computation for our deterministic model, it is equivalent to replace the numerator by the shadow price of the transition equation of atmospheric carbon concentration at year t , and the denominator by the shadow price of the regional capital transition equation.

We define the regional noncooperative SCC as

$$\tau_{t,i}^{\text{OLNE}} = -1000 \left(\frac{\partial V_{t,i}^{\text{OLNE}}}{\partial M_t^{\text{AT}}} \right) / \left(\frac{\partial V_{t,i}^{\text{OLNE}}}{\partial K_{t,i}} \right)$$

where $V_{t,i}^{\text{OLNE}} = \max_{c_{s,i}, \mu_{s,i}} \sum_{s=t}^{\infty} \beta^t u(c_{s,i})L_{s,i}$ is the optimal regional welfare starting from year t with a given starting state vector $(K_{t,1}, K_{t,2}, M_t^{\text{AT}}, \dots)$ under OLNE. In its computation, it is equivalent to replace the numerator by the shadow price of the transition equation of atmospheric carbon concentration at year t , and the denominator by the shadow price of the regional capital transition equation, for each economic region $i = 1, 2$.

4 Results

We first report the results in the baseline case. Figure 5 shows paths of regional SCC (the left panel) and optimal regional carbon taxes (the right panel) in the economic regions in a cooperative or noncooperative world. The initial cooperative SCC for the North is very high (\$806/tCO₂), 6.9 times the initial cooperative SCC for the Tropic/South (\$117/tCO₂), although the North experiences little impact on its economic growth from climate change in this century according to the GDP scenario 1 as shown in Figure 3. It is not surprising that the North has such a large SCC under cooperation, because consumption in the poor countries in the Tropic/South has higher marginal utility than the rich countries in the North, and then the social planner uses differentiated carbon taxes to achieve some second-best redistribution, under our assumption that there is no direct transfers of physical consumption or investment goods between the regions.¹⁷ Moreover, the cooperative SCC for the North is much larger than the cooperative optimal regional carbon tax for the North, because the emission control rate for the North has hit the upper bound, 1, since the initial period. That is, under cooperation the North would have zero emissions since the first period, while the Tropic/South would have zero emissions since 2050. The large cooperative SCC or carbon taxes of the North cannot be regarded as a realistic policy proposal since there are very few unselfish and completely cooperative sovereigns in the real world. However, this polar cooperative world provides an insight into the structure of optimal carbon taxes. This structure suggests that when the rich countries in the North are cooperative it is optimal for them to reduce emissions in a much more stringent way than the poor countries in the Tropic/South in order to help maximize the global welfare, as otherwise the Tropic/South would have much more damages from climate change so that the global welfare would be reduced significantly. This behavior leads to very high cooperative SCC or carbon taxes in the North.

The noncooperative SCC for the North is dramatically reduced to be \$49 in the first period, and then gradually increases. Moreover, Figure 5 shows that the whole path of SCC or carbon taxes for the North in the noncooperative world is dramatically lower than in the cooperative world. But note that the numbers of SCC are relatively not small in comparison with the existing literature. For example, in DICE-2016R the global SCC in 2015 is only \$31, much smaller than our regional SCC even under noncooperation. This

¹⁷If we allow direct transfers of consumption and capital investment without any border friction costs under cooperation, then the regional SCC is the same across the regions. For example, the initial SCC becomes \$259 for both economic regions, much lower than the average of \$806 and \$117 or their population weighted average (\$381), due to the lower marginal utility in the richer Tropic under the free allocation of consumption and capital investment.

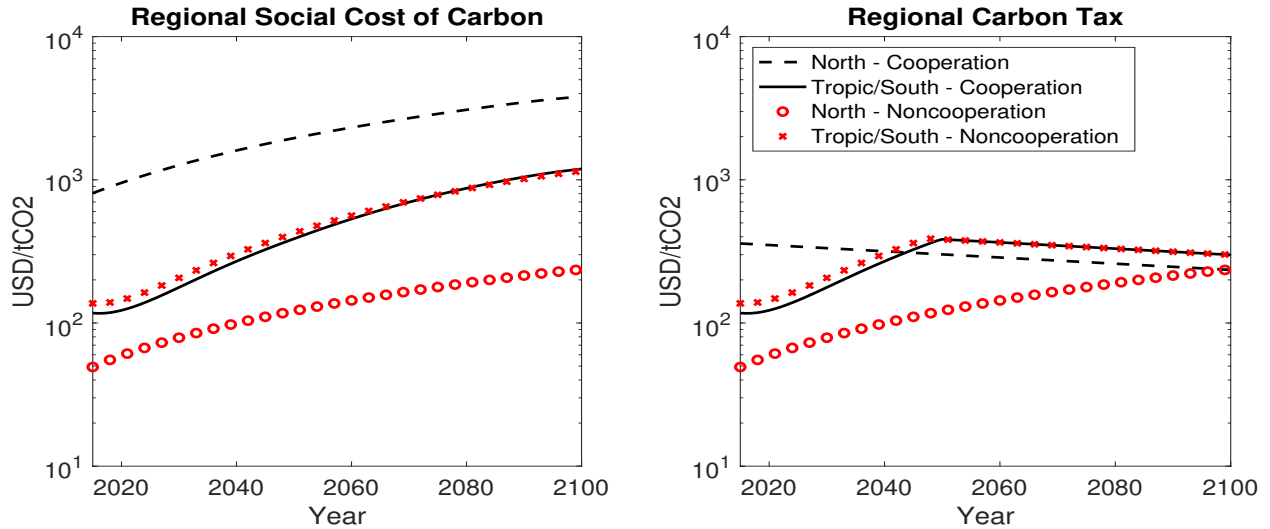


Figure 5: Regional SCC and optimal regional carbon taxes under climate damage in the baseline case. Left panel: regional SCC; Right panel: optimal carbon tax; Black lines: cooperative results; Red lines: noncooperative results; Dashed lines: solution for the North under cooperation; Solid lines: solution for the Tropic/South under cooperation; Circled lines: solution for the North under noncooperation; Marked lines: solution for the Tropic/South under noncooperation.

is because the quadratic damage function in DICE-2016R has a much smaller coefficient than ours, then much smaller damages under the same temperature. For example, if the global and regional temperature increase over the initial year is 1°C , then in DICE-2016R the global temperature anomaly is 1.85°C and reduces contemporaneous output by 0.8% (the temperature anomaly has no lagged effect in future output), but our TFP model 1 estimates 1.2% reduction of contemporaneous output in the North and 12.1% reduction in the Tropic/South and the temperature anomaly has lagged effect in the next 10 years' output. Moreover, the nonlinearity in our TFP models is much larger. For example, if the temperature increase over the initial year is 2°C , then the damage estimate in DICE-2016R is 1.9% of contemporaneous output, but ours are 3.2% in the North and 39.1% in the Tropic while there is still lagged effects in future output. For the Tropic/South, its initial noncooperative SCC or carbon tax increases to \$137, 17% higher than in the cooperative world, but since 2076 its noncooperative SCC is also slightly lower than in the cooperative world.¹⁸ Therefore, even under noncooperation, both economic regions should take stringent climate policy.

¹⁸Since the emission control rates do not hit their upper bound before 2050 in the Tropic/South under cooperation or noncooperation, the regional optimal carbon tax path is identical to the regional noncooperative SCC path for the Tropic/South before 2050 as shown in Figure 5. With the same reason, the North has the identical paths between SCC and carbon tax under noncooperation in the whole century.

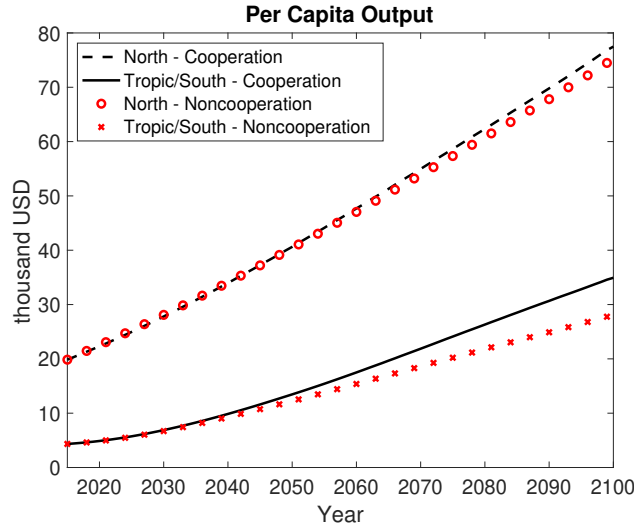


Figure 6: Regional per capita output under cooperation and noncooperation in the baseline case

The main driver of these high regional SCC or carbon taxes is that we incorporate the serious climate damage to economic growth in the Tropic/South. Figure 6 shows that in our model with optimal climate policy, the per capita output of the Tropic/South in 2100 is \$34,927 in the cooperative world or \$28,021 in the noncooperative world, while the per capita output of the North in 2100 is \$77,484 under cooperation, or \$75,091 under noncooperation. That is, relative to cooperation, noncooperation reduces output by an extra 3.1% (i.e., \$2,393 per capita) in the North, but reduces output by a substantially extra 20% (i.e., \$6,907 per capita) in the Tropic/South in 2100.

Figure 7 displays paths of regional atmospheric temperature anomalies. Under cooperation, with the most stringent climate policy shown in Figure 5, the atmospheric temperature anomaly is 2.1°C in the North, 1.3°C in the Tropic, and 1.1°C in the South, and the global average is below 1.5°C. But with the noncooperative but still stringent climate policy, in 2100 the atmospheric temperature anomaly is 2.7°C in the North, 1.8°C in the Tropic, and 1.4°C in the South, and the global average is below 2.0°C. Thus, the temperature anomalies are compatible with the SSP1 population scenario that is used in our calibration.

4.1 Impact of Damage Estimates

We run the cases 2-5 to test the impact of damage estimates with the TFP models 1-2. Figure 8 displays the regional SCC under cooperation or noncooperation and shows the similar pattern of the left panel of Figure 5: the North in the cooperative world (the top-left panel) has the largest SCC for each case, in comparison with the North under

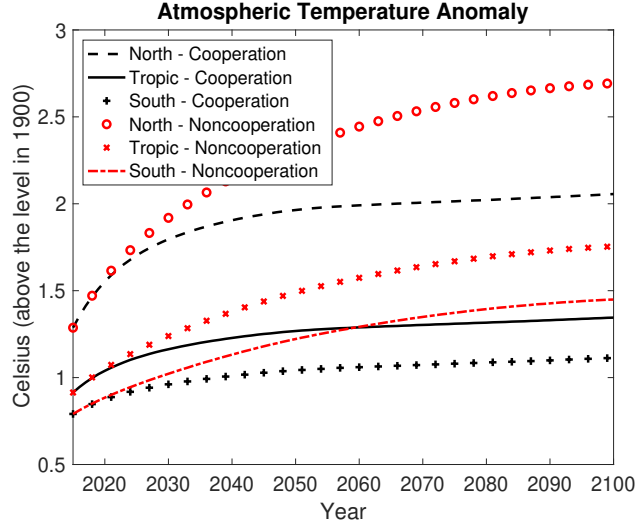


Figure 7: Atmospheric temperature anomaly under climate damage in the baseline case.

noncooperation (the bottom-left panel) or the Tropic/South (the right panels). In the North (the left panels), the cases 5-6 have larger SCC than the other cases when comparing among three solid lines only (associated with the TFP model 1) or comparing among three dashed lines only (associated with the TFP model 2), because the North has the larger loss in the GDP scenario 3 (associated with the cases 5-6). Similarly, in the Tropic/South the cases 5-6 have the larger SCC under cooperation but not under noncooperation, because both economic regions have large climate damage in the GDP scenario 3 but the Tropic/South has smaller damage than in the GDP scenario 1 (associated with the cases 1-2). Comparing the solid lines with the dashed lines under the same color (a different color represents a different GDP scenario for calibration), we see the climate effect on TFP growth leads to larger SCC in the initial periods than the ten-year lagged effect on TFP levels, but smaller SCC in later periods. This occurs because the climate effect on TFP growth is permanent, so both economic regions want to impose more stringent climate policy at earlier periods such that the temperature anomaly is well controlled and then has less damage and smaller SCC in later periods.

Figure 9 displays the per capita output in the case 5.¹⁹ Figure 9 shows that noncooperation causes only little extra loss in each economic region, in comparison to the cooperative solution. While it looks a bit weird, this occurs because under either cooperation or noncooperation, both economic regions hit the upper bound of the emission control rates soon with small time differences between cooperative and noncooperative solutions. For example, the Tropic/South hits the upper bound in 2044 and 2049, under cooperation and nonco-

¹⁹We omit the other cases because the cases 2-4' figures are similar to Figure 6 and the case 6's figure is similar to Figure 9.

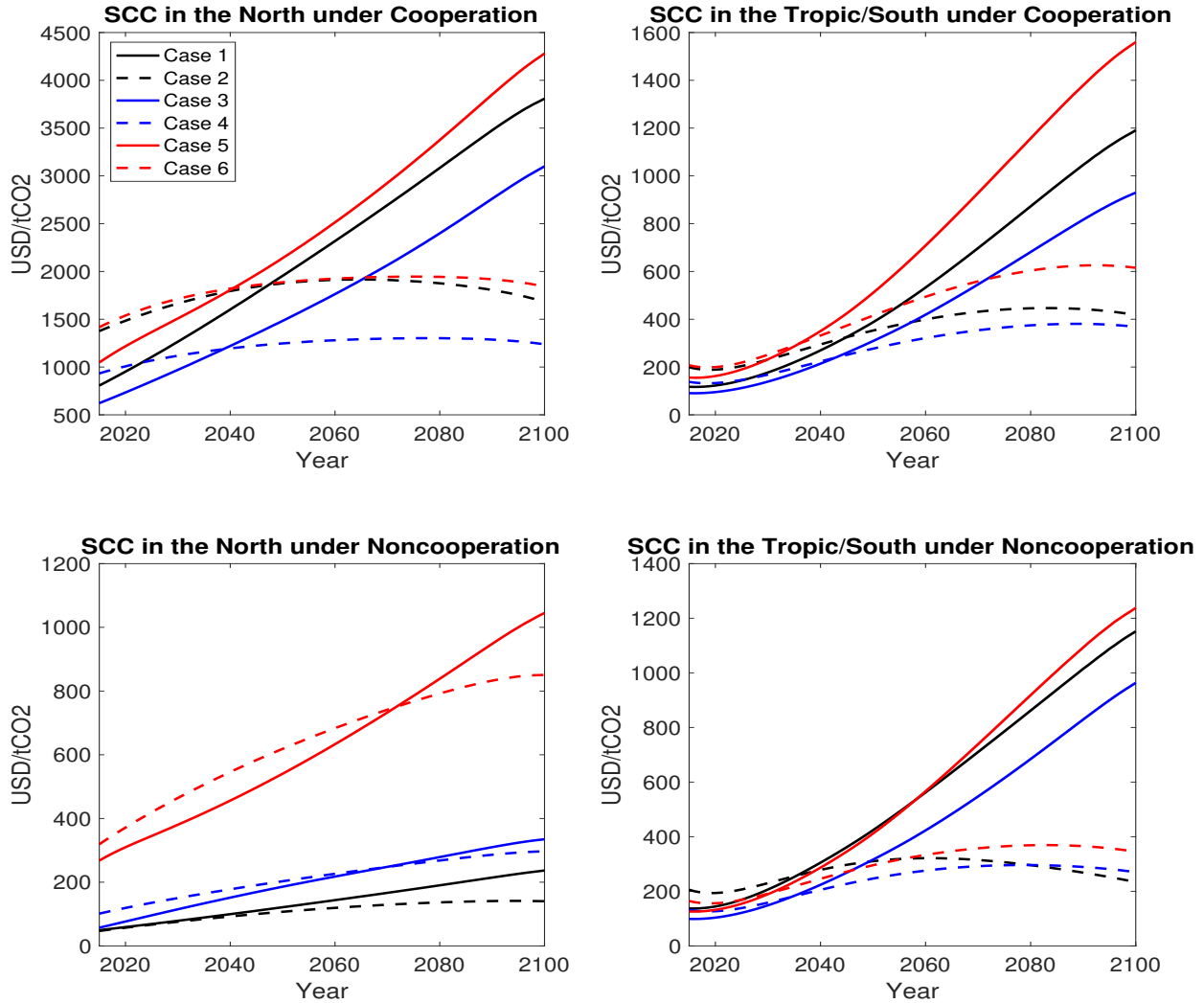


Figure 8: Regional SCC in the cases 1-6 under cooperation or noncooperation. Black lines: Cases 1-2 with the GDP scenario 1 for calibration; Blue lines: Cases 3-4 with the GDP scenario 2 for calibration; Red lines: with the GDP scenario 3 for calibration. Solid lines: TFP model 1's solutions; Dashed lines: TFP model 2's solutions.

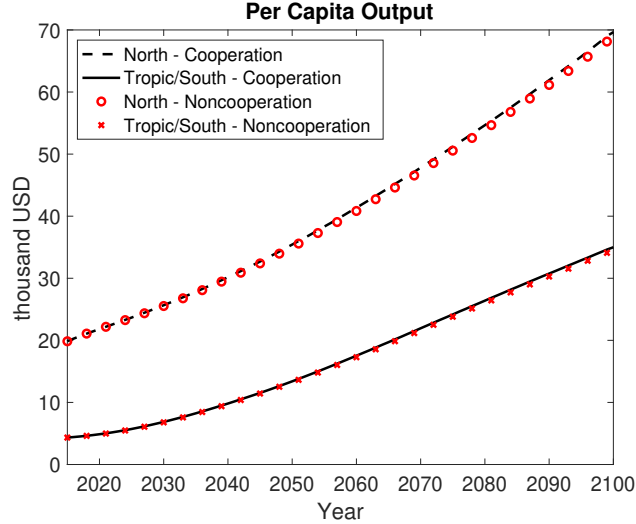


Figure 9: Regional per capita GDP in the case 5 under cooperation and noncooperation

operation respectively. Thus, although the SCC is high (and higher than the cases 1 and 3 from Figure 8), it cannot affect the temperature, as only the emission control rates can. That is, there is little difference in emissions between cooperation and noncooperation, so it has little difference in temperature anomaly, then little difference in climate damage, and finally little difference in output: noncooperation reduces output by an extra 1.2% (i.e., \$870 per capita) in the North, and by an extra 1.6% (i.e., \$548 per capita) in the Tropic/South in 2100, in comparison to the cooperative solution. Note that the small difference between cooperative and noncooperative solutions happens because the huge climate damage in both economic regions forces them to adopt extremely stringent climate policy to control carbon emissions even without cooperation. That is, no matter whether to choose cooperation or noncooperation, both economic regions should choose very stringent climate policy.

Table 1 lists the initial SCC and per capita output in 2100 for all six cases. We see that in comparison with the ten-year lagged effect on TFP levels, the climate effect on the TFP growth leads to much larger SCC in 2015 in both economic regions under cooperation, and in the Tropic/South under noncooperation, although both TFP models are calibrated with the same GDP scenarios. This happens because the impact on TFP growth is permanent on all future TFP, but the impact on TFP levels is not, although both influences GDP growth. Moreover, the smallest SCC in the initial period, \$47/tCO₂, in the North under noncooperation in the case 2, is still not small in comparison with the existing literature (e.g., in DICE 2016R the global SCC in 2015 is only \$31), while the highest initial SCC is up to \$319 in the North under noncooperation, \$206 in the Tropic/South under noncooperation, \$1,417 in the North under cooperation, or \$207 in the Tropic/South under cooperation.

Table 1 also tells us that noncooperation causes an extra reduction in output for both

Case	SCC in 2015 (\$/tCO ₂)				per capita output in 2100			
	Cooperation		Noncooperation		Cooperation		Noncooperation	
	North	T/S	North	T/S	North	T/S	North	T/S
1	806	117	49	137	77,484	34,927	75,091	28,021
2	1,376	199	47	206	78,267	30,104	76,004	23,285
3	622	91	57	99	80,660	35,432	78,397	32,077
4	933	138	101	132	75,091	32,779	72,089	29,490
5	1,048	156	268	126	69,653	34,993	68,782	34,445
6	1,417	207	319	164	66,825	31,573	65,259	30,871

Table 1: SCC in 2015 and per capita output in 2100. “T/S” means the Tropic/South.

economic regions for all cases in comparison to the cooperative solution, while loss in the Tropic/South is large in the cases 1-4. Moreover, Table 1 shows that there is no significant difference in the Tropic/South’s SCC between cooperation and noncooperation, while the difference is significant in the North, as the Tropic/South will suffer a large loss from climate change while the North will not. But here we also ignore the spillover effects of international trade, migration and social conflict between regions in our model, so the North might suffer a larger loss in output, particularly under noncooperation (see e.g. Burke et al. 2015a; Carleton and Hsiang 2016; Mach et al. 2019; Kortum and Weisbach 2021).

Except the above analysis with different TFP models calibrated from different climate damage estimates (i.e., GDP scenarios), we also do sensitivity analysis over 0.25, 0.5, or 0.75 times the calibrated values of both $\zeta_{i,1}^{\text{TFP}}$ and $\zeta_{i,2}^{\text{TFP}}$ in the baseline case for both $i = 1, 2$. Figure 10 shows that the initial regional SCCs are almost linear to the levels of impact in each economic region under cooperation or noncooperation. For instance, if we reduce the impact parameters, $\zeta_{i,1}^{\text{TFP}}$ and $\zeta_{i,2}^{\text{TFP}}$, to their half values in the economic regions, then the initial regional SCCs are also nearly half: \$424 for the North and \$62 for the Tropic/South under cooperation; or \$26 for the North and \$76 for the Tropic/South under noncooperation. Moreover, this almost linear relation also holds in later years until 2050.

4.2 Bias from Ignoring Climate Feedbacks and Heat Transfer

If we ignore climate feedbacks and heat transfer between the regions (i.e., let $\xi_4 = \xi_6 = \xi_7 = 0$), then the regional SCC will become significantly lower in the economic regions. Under cooperation the initial regional SCC is down to \$431 in the North or \$63 in the Tropic/South, about 54% the initial regional SCC in the North or correspondingly in the Tropic/South in the baseline case with climate feedbacks and heat transfer. Under noncooperation ignoring climate feedbacks and heat transfer also significantly decreases the initial regional SCC to \$14 in the North or \$87 in the Tropic/South. Figure 11 shows our solutions under cooperation

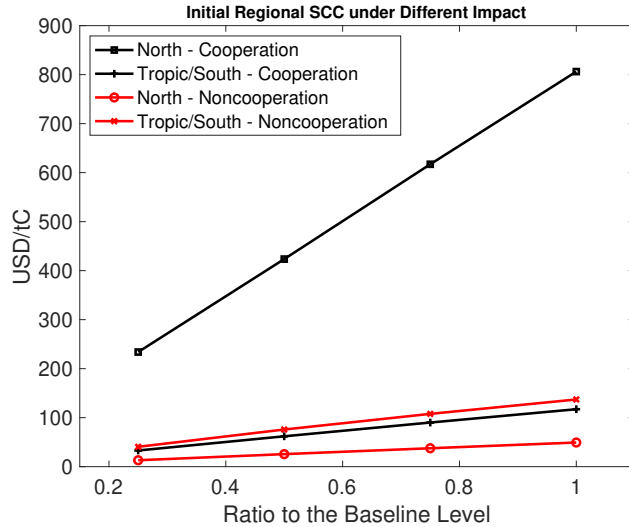


Figure 10: Initial regional SCC under different levels of impact

or noncooperation with the assumption that there is no climate feedback nor heat transfer. The left panel of Figure 11 displays the SCC in this century, which has the similar pattern with the baseline case but much smaller values. That is, ignoring climate feedbacks and heat transfer leads to significant underestimation of regional SCC. This happens because ignoring climate feedbacks cools down the atmospheric temperature in the North and the Tropic, and thus reduces its damage: in 2100 the per-capita output is \$80,007 in the North under cooperation, \$38,063 in the Tropic/South under cooperation, \$79,050 in the North under noncooperation, or \$29,468 in the Tropic/South under noncooperation, so they are higher than in the baseline case with climate feedbacks and heat transfer. The right panel of Figure 11 shows that if climate feedbacks and heat transfer were not present, atmospheric temperature anomalies in the three regions would merge after 30 years, and the global mean atmospheric temperature is lower than in the baseline case. Moreover, heat transport from low latitudes to high latitudes may increase sea level rise, permafrost melt and climate tipping risks causing damages in the low latitudes with additional effects on regional SCCs and temperatures (Brock and Xepapadeas, 2017; Cai et al., 2019). Thus, ignoring climate feedbacks and heat transfer may have larger bias in underestimating the SCCs.

5 Discussion and Conclusion

The regional SCC and the impact of climate change on GDP are well-researched issues in the economics of climate change. The present paper using a three-region model provides new insights on two issues that, as far as we know, have not been addressed simultaneously

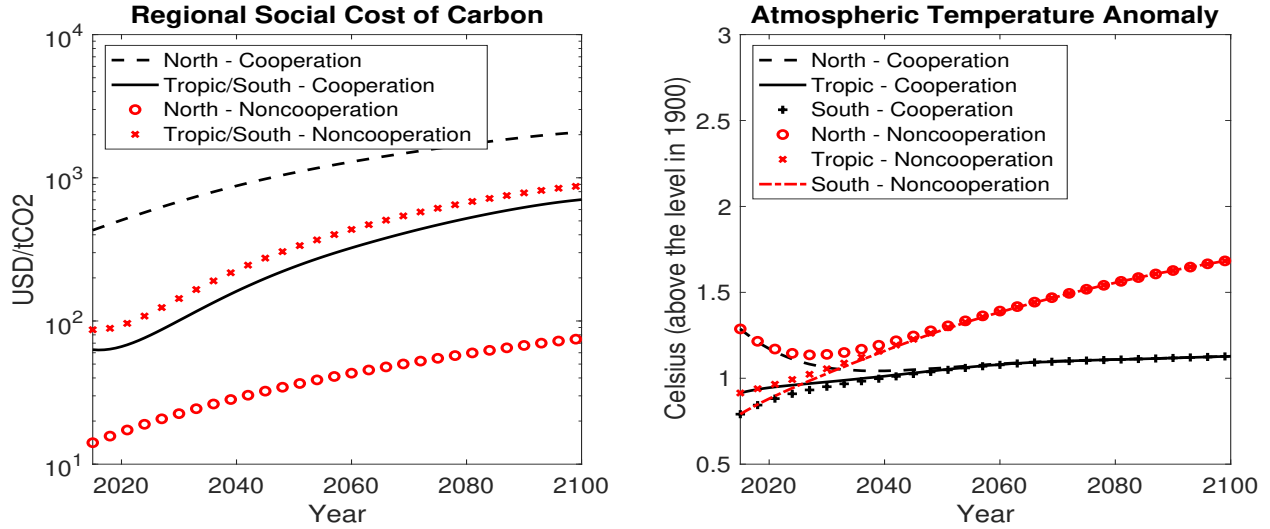


Figure 11: Regional SCC and Atmospheric Temperature Anomaly without Heat Transfer nor Climate Feedbacks.

before in this context: the effect on regional SCC under cooperation or noncooperation when climate change impacts economic growth, and the impact of heat transfer on regional climate policies. First, we find that whether there is cooperation or noncooperation, it is always optimal for economic regions to choose stringent climate policies and keep the global mean temperature anomaly in this century below 1.5°C under cooperation or 2°C under noncooperation. Second, we show the difference in regional SCC associated with a cooperative or noncooperative world. Our results suggest that a shift towards cooperation in international climate change policy will result in substantially higher regional SCCs for the developed North relatively to the developing Tropic/South, and substantively higher GDP per capita for the Tropic with a small increase in GDP per capita for the North. Third, if climate change affects TFP growth instead of the TFP level, then our results, which are in line with recent literature, indicate that damages and therefore regional SCCs are much higher except for the noncooperative SCC in the North.

Given the uncertainty surrounding the specification and the parameterization of the damage function in IAMs and the strong critique of the traditional damage functions which are associated with level, not growth, effects, our results suggest that for an efficient climate policy the issue of whether climate change affects levels or growth or both needs to be seriously addressed. Finally, we explicitly show that ignoring climate feedbacks and heat transport from the equator to the North introduces serious bias in the calculation of optimal carbon taxes. This result provides more insights into the ways that optimal climate policies should be designed when well-documented results of climate science, such as climate feedbacks and damage functions, are considered.

This paper has certain limitations. For example, it has not discussed the spillover effects of international trade, migration and social conflict between regions, which might have significant impact on the optimal climate policy, particularly in the North. A finer spatial resolution or more realistic economic regions would also play an important role.

References

- Maximilian Auffhammer. Quantifying Economic Damages from Climate Change. *Journal of Economic Perspectives*, 32(4):33–52, 2018.
- Michael Barnett, William Brock, and Lars Peter Hansen. Pricing Uncertainty Induced by Climate Change. *The Review of Financial Studies*, 33(3):1024–1066, 2020.
- Michael Barnett, William Brock, and Lars P. Hansen. Climate Change Uncertainty Spillover in the Macroeconomy. Working Paper 29064, National Bureau of Economic Research, 2021. URL <https://www.nber.org/papers/w29064>.
- Alan Barreca, Karen Clay, Olivier Deschenes, Michael Greenstone, and Joseph S. Shapiro. Adapting to climate change: The remarkable decline in the US temperature-mortality relationship over the twentieth century. *Journal of Political Economy*, 124(1):105–159, 2016.
- W. Brock and A. Xepapadeas. Climate change policy under polar amplification. *European Economic Review*, 94:263–282, 2017.
- William Brock and Anastasios Xepapadeas. Regional Climate Change Policy Under Positive Feedbacks and Strategic Interactions. *Environmental and Resource Economics*, 72(1): 51–75, 2019.
- Marshall Burke, Solomon M. Hsiang, and Edward Miguel. Climate and Conflict. *Annual Review of Economics*, 7(1):577–617, 2015a.
- Marshall Burke, Solomon M. Hsiang, and Edward Miguel. Global non-linear effect of temperature on economic production. *Nature*, 527(7577):235–239, 2015b.
- Marshall Burke, W. Matthew Davis, and Noah S. Diffenbaugh. Large potential reduction in economic damages under UN mitigation targets. *Nature*, 557(7706):549–553, 2018.
- Yongyang Cai. The Role of Uncertainty in Controlling Climate Change. *Oxford Research Encyclopedia of Economics and Finance*, 2021. doi: 10.1093/acrefore/9780190625979.013.573.
- Yongyang Cai and Thomas S. Lontzek. The social cost of carbon with economic and climate risks. *Journal of Political Economy*, 6:2684–2734, 2019.

- Yongyang Cai, Timothy M. Lenton, and Thomas S. Lontzek. Risk of multiple interacting tipping points should encourage rapid CO2 emission reduction. *Nature Climate Change*, 6(5):520–525, 2016.
- Yongyang Cai, Kenneth L. Judd, and Thomas S. Lontzek. The social cost of carbon with economic and climate risks. Hoover economics working paper 18113, 2017. URL <https://www.hoover.org/research/social-cost-carbon-economic-and-climate-risk>.
- Yongyang Cai, William Brock, Anastasios Xepapadeas, and Kenneth L. Judd. Climate policy under spatial heat transport: Cooperative and noncooperative regional outcomes. arXiv preprint 1909.04009, 2019. URL <https://arxiv.org/abs/1909.04009>.
- Tamma A. Carleton and Solomon M. Hsiang. Social and economic impacts of climate. *Science*, 353(6304), 2016.
- Melissa Dell, Benjamin F. Jones, and Benjamin A. Olken. Temperature shocks and economic growth: Evidence from the last half century. *American Economic Journal: Macroeconomics*, 4(3):66–95, 2012.
- Francis Dennig, Mark B. Budolfson, Marc Fleurbaey, Asher Siebert, and Robert H. Socolow. Inequality, climate impacts on the future poor, and carbon prices. *Proceedings of the National Academy of Sciences*, 112(52):15827–15832, 2015.
- Klaus Desmet and Esteban Rossi-Hansberg. On the spatial economic impact of global warming. *Journal of Urban Economics*, 88:16–37, 2015.
- Klaus Desmet, Robert E. Kopp, Scott A. Kulp, David Krisztian Nagy, Michael Oppenheimer, Esteban Rossi-Hansberg, and Benjamin H. Strauss. Evaluating the Economic Cost of Coastal Flooding. *American Economic Journal: Macroeconomics*, 13(2):444–486, 2021.
- Simon Dietz and Nicholas Stern. Endogenous growth, convexity of damage and climate risk: How nordhaus’ framework supports deep cuts in carbon emissions. *The Economic Journal*, 125(583):574–620, 2015.
- Simon Dietz and Frank Venmans. Cumulative carbon emissions and economic policy: In search of general principles. *Journal of Environmental Economics and Management*, 96: 108–129, 2019.
- Simon Dietz, James Rising, Thomas Stoerk, and Gernot Wagner. Economic impacts of tipping points in the climate system. *Proceedings of the National Academy of Sciences*, 118(34):e2103081118, 2021a.

- Simon Dietz, Frederick van der Ploeg, Armon Rezai, and Frank Venmans. Are Economists Getting Climate Dynamics Right and Does It Matter? *Journal of the Association of Environmental and Resource Economists*, 8(5):895–921, 2021b.
- Noah S. Diffenbaugh and Marshall Burke. Global warming has increased global economic inequality. *Proceedings of the National Academy of Sciences*, 116(20):9808–9813, 2019.
- Prajit K. Dutta and Roy Radner. A strategic analysis of global warming: Theory and some numbers. *Journal of Economic Behavior & Organization*, 71(2):187–209, 2009.
- Mikhail Golosov, John Hassler, Per Krusell, and Aleh Tsyvinski. Optimal taxes on fossil fuel in general equilibrium. *Econometrica*, 82(1):41–88, 2014.
- John Hassler and Per Krusell. Economics and climate change: integrated assessment in a multi-region world. *Journal of the European Economic Association*, 10(5):974–1000, 2012.
- Geoffrey Heal and Jisung Park. Reflections—Temperature Stress and the Direct Impact of Climate Change: A Review of an Emerging Literature. *Review of Environmental Economics and Policy*, 10(2):347–362, 2016.
- Solomon Hsiang, Robert Kopp, Amir Jina, James Rising, Michael Delgado, Shashank Mohan, D. J. Rasmussen, Robert Muir-Wood, Paul Wilson, Michael Oppenheimer, Kate Larsen, and Trevor Houser. Estimating economic damage from climate change in the united states. *Science*, 356(6345):1362–1369, 2017.
- Niko Jaakkola and Frederick van der Ploeg. Non-cooperative and cooperative climate policies with anticipated breakthrough technology. *Journal of Environmental Economics and Management*, 97:42–66, 2019.
- Matthew E. Kahn, Kamiar Mohaddes, Ryan N. C. Ng, M. Hashem Pesaran, Mehdi Raissi, and Jui-Chung Yang. Long-term macroeconomic effects of climate change: A cross-country analysis. *Energy Economics*, 104:105624, 2021.
- Matthias Kalkuhl and Leonie Wenz. The impact of climate conditions on economic production. Evidence from a global panel of regions. *Journal of Environmental Economics and Management*, 103:102360, 2020.
- Samir Kc and Wolfgang Lutz. The human core of the shared socioeconomic pathways: Population scenarios by age, sex and level of education for all countries to 2100. *Global Environmental Change*, 42:181–192, 2017.

- Charles D. Kolstad and Frances C. Moore. Estimating the Economic Impacts of Climate Change Using Weather Observations. *Review of Environmental Economics and Policy*, 14(1):1–24, 2020.
- Samuel S. Kortum and David A. Weisbach. Optimal Unilateral Carbon Policy. SSRN Scholarly Paper ID 3958930, Social Science Research Network, Rochester, NY, November 2021. URL <https://papers.ssrn.com/abstract=3958930>.
- Per Krusell and Anthony Smith. Climate change around the world. memo, 2017.
- Peter L. Langen and Vladimir A. Alexeev. Polar amplification as a preferred response in an idealized aquaplanet gcm. *Climate Dynamics*, 29(2):305–317, 2007.
- Martin Leduc, H. Damon Matthews, and Ramon de Elia. Regional estimates of the transient climate response to cumulative CO₂ emissions. *Nature Climate Change*, 6(5):474–478, 2016.
- Katharine J. Mach, Caroline M. Kraan, W. Neil Adger, Halvard Buhaug, Marshall Burke, James D. Fearon, Christopher B. Field, Cullen S. Hendrix, Jean-Francois Maystadt, John O’Loughlin, Philip Roessler, Jurgen Scheffran, Kenneth A. Schultz, and Nina von Uexkull. Climate as a risk factor for armed conflict. *Nature*, 571(7764):193–197, 2019.
- Linus Mattauch, H. Damon Matthews, Richard Millar, Armon Rezai, Susan Solomon, and Frank Venmans. Steering the Climate System: Using Inertia to Lower the Cost of Policy: Comment. *American Economic Review*, 110(4):1231–1237, 2020.
- H. Damon Matthews, Nathan P. Gillett, Peter A. Stott, and Kirsten Zickfeld. The proportionality of global warming to cumulative carbon emissions. *Nature*, 459(7248):829–832, 2009.
- M. Meinshausen, S.C.B. Raper, and T.M.L. Wigley. Emulating coupled atmosphere-ocean and carbon cycle models with a simpler model, magicc6: Part I - model description and calibration. *Atmospheric Chemistry and Physics*, 11:1417–1452, 2011a.
- M. Meinshausen, S.J. Smith, K. Calvin, J.S. Daniel, M.L.T. Kainuma, J-F. Lamarque, K. Matsumoto, S.A. Montzka, S.C.B. Raper, K. Riahi, A. Thomson, G.J.M. Velders, and D.P.P. van Vuuren. The RCP greenhouse gas concentrations and their extensions from 1765 to 2300. *Climatic Change*, 109:213–241, 2011b.
- Frances C. Moore and Delavane B. Diaz. Temperature impacts on economic growth warrant stringent mitigation policy. *Nature Climate Change*, 5(2):127–131, 2015.

- Elisabeth J. Moyer, Mark D. Woolley, Nathan J. Matteson, Michael J. Glotter, and David A. Weisbach. Climate impacts on economic growth as drivers of uncertainty in the social cost of carbon. *The Journal of Legal Studies*, 43(2):401–425, 2014.
- Carlos Navarro-Racines, Jaime Tarapues, Philip Thornton, Andy Jarvis, and Julian Ramirez-Villegas. High-resolution and bias-corrected CMIP5 projections for climate change impact assessments. *Scientific Data*, 7(1):7, 2020.
- James E. Neumann, Jacqueline Willwerth, Jeremy Martinich, James McFarland, Marcus C. Sarofim, and Gary Yohe. Climate Damage Functions for Estimating the Economic Impacts of Climate Change in the United States. *Review of Environmental Economics and Policy*, 14(1):25–43, 2020.
- Richard G. Newell, Brian C. Prest, and Steven E. Sexton. The GDP-Temperature relationship: Implications for climate change damages. *Journal of Environmental Economics and Management*, 108:102445, 2021.
- W. D. Nordhaus. Revisiting the social cost of carbon. *Proceedings of the National Academy of Sciences of the United States of America*, 114(7):1518–1523, 2017a.
- William D. Nordhaus. *A Question of Balance: Weighing the Options on Global Warming Policies*. Yale University Press, 2008.
- William D. Nordhaus. Economic aspects of global warming in a post-copenhagen environment. *Proceedings of the National Academy of Sciences*, 107(26):11721–11726, 2010.
- William D. Nordhaus. Revisiting the social cost of carbon. *Proceedings of the National Academy of Sciences*, 114(7):1518–1523, 2017b.
- William D. Nordhaus and Zili Yang. A regional dynamic general equilibrium model of alternative climate change strategies. *The American Economic Review*, 86(4):741–765, 1996.
- Armon Rezai, Lance Taylor, and Duncan Foley. Economic growth, income distribution, and climate change. *Ecological Economics*, 146:164 – 172, 2018.
- Keywan Riahi, Detlef P. van Vuuren, Elmar Kriegler, Jae Edmonds, Brian C. ... O’Neill, and Massimo Tavoni. The Shared Socioeconomic Pathways and their energy, land use, and greenhouse gas emissions implications: An overview. *Global Environmental Change*, 42:153–168, 2017.

- Katharine Ricke, Laurent Drouet, Ken Caldeira, and Massimo Tavoni. Country-level social cost of carbon. *Nature Climate Change*, 8(10):895, 2018.
- Malte F. Stuecker, Cecilia M. Bitz, Kyle C. Armour, Cristian Proistosescu, Sarah M. Kang, Shang-Ping Xie, Doyeon Kim, Shayne McGregor, Wenjun Zhang, Sen Zhao, Wenju Cai, Yue Dong, and Fei-Fei Jin. Polar amplification dominated by local forcing and feedbacks. *Nature Climate Change*, 8(12):1076–1081, 2018.
- Frederick van der Ploeg. The safe carbon budget. *Climatic Change*, 147(1):47–59, 2018.
- Frederick van der Ploeg and Aart de Zeeuw. Non-cooperative and cooperative responses to climate catastrophes in the global economy: A north-south perspective. *Environmental and Resource Economics*, 65(3):519–540, 2016.
- Martin L. Weitzman. GHG targets as insurance against catastrophic climate damages. *Journal of Public Economic Theory*, 14(2):221–244, 2012.
- Carl Wunsch. The Total Meridional Heat Flux and Its Oceanic and Atmospheric Partition. *Journal of Climate*, 18(21):4374–4380, 2005.

Appendix

A.1 Carbon Cycle and Its Calibration

The carbon cycle dynamics is

$$\mathbf{M}_{t+1} = \Phi_{\mathbf{M}} \mathbf{M}_t + (E_t, 0, 0)^\top, \quad (\text{A.1})$$

where the transition matrix of the carbon cycle is

$$\Phi_{\mathbf{M}} = \begin{bmatrix} 1 - \phi_{12} & \phi_{12} M_*^{\text{AT}} / M_*^{\text{UO}} & & \\ \phi_{12} & 1 - \phi_{21} - \phi_{23} & \phi_{23} M_*^{\text{UO}} / M_*^{\text{DO}} & \\ & \phi_{23} & 1 - \phi_{23} M_*^{\text{UO}} / M_*^{\text{DO}} & \\ & & & \end{bmatrix} \quad (\text{A.2})$$

where M_*^{AT} , M_*^{UO} , M_*^{DO} are pre-industrial carbon concentrations in the atmosphere, the upper ocean and the deep ocean. MAGICC 6 (Meinshausen et al., 2011a) provides four global RCP scenarios, i.e., RCP2.6, RCP4.5, RCP6 and RCP8.5, which include both emission paths and carbon concentration in the atmosphere. The parameters ϕ_{12} and ϕ_{23} are calibrated against the four RCP scenarios. That is, we solve the following minimization problem:

$$\min_{\phi_{12}, \phi_{23}} \sum_{j=1}^4 \sum_{t=0}^{85} \left| M_t^{\text{AT},j} / M_t^{\text{MAGICC,AT},j} - 1 \right|$$

subject to the carbon cycle system (A.1) for each RCP scenario $j = 1, \dots, 4$ (represented in the subscript) over the 85-year time horizon (from the initial year 2015 to 2100). Here the subscript ‘‘MAGICC’’ represents the data from MAGICC 6, and the global CO₂ emissions E_t for each RCP scenario are also given by MAGICC 6. Figure A.1 shows that our calibrated carbon cycle can approximate well for all scenarios.

A.2 Solve Open-loop Nash Equilibrium

We follow Nordhaus and Yang (1996) to use an iterative method to solve the open-loop Nash equilibrium. We use the social planner’s solution as the initial guess of two regional emission paths, denoted as $\{E_{t,i}^{\text{Ind},0} : t = 0, 1, \dots, T\}$ for economic region $i = 1, 2$, where $T = 500$ years. Now we assume the region 2’s emission path is fixed at $E_{t,2}^{\text{Ind},0}$, and solve the region 1’s social

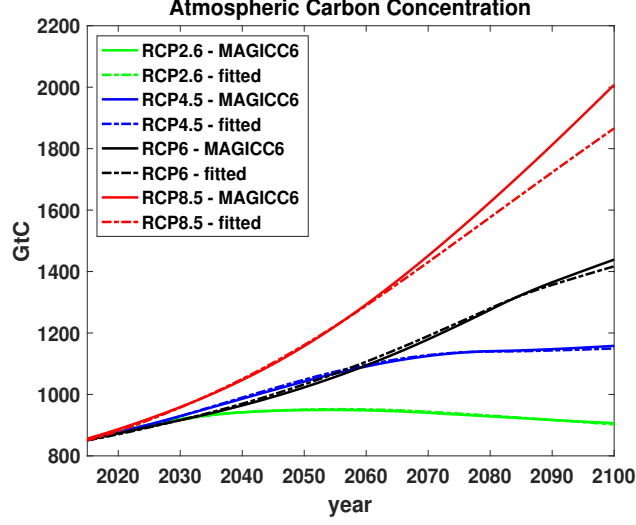


Figure A.1: Fitting the Carbon Cycle to Match RCP scenarios

planner problem:

$$\max_{c_{t,1}, \mu_{t,1}} \sum_{t=0}^{\infty} \beta^t u(c_{t,1}) L_{t,1}, \quad (\text{A.3})$$

subject to the transition laws of three carbon concentration levels, four temperature levels, and its own regional capital, while the global emission is assumed to be

$$E_t = E_{t,1}^{\text{Ind}} + E_{t,2}^{\text{Ind},0} + E_t^{\text{Land}}.$$

Note that $E_{t,1}^{\text{Ind}}$ is endogenous but $E_{t,2}^{\text{Ind},0}$ is exogenous. The solution of $E_{t,1}^{\text{Ind}}$ is denoted $E_{t,1}^{\text{Ind},*}$. Similarly, we assume the region 1's emission path is fixed at $E_{t,1}^{\text{Ind},0}$, and solve the region 2's social planner problem, and obtain its solution of $E_{t,2}^{\text{Ind}}$, denoted $E_{t,2}^{\text{Ind},*}$. Now we let

$$E_{t,i}^{\text{Ind},1} = \omega E_{t,i}^{\text{Ind},*} + (1 - \omega) E_{t,i}^{\text{Ind},0}$$

for all t and i , where ω is chosen to be 0.5. Thus, we have updated the emission paths $\{E_{t,i}^{\text{Ind},0} : t = 0, 1, \dots, T\}$ to $\{E_{t,i}^{\text{Ind},1} : t = 0, 1, \dots, T\}$. Similarly we can use $\{E_{t,i}^{\text{Ind},1} : t = 0, 1, \dots, T\}$ to generate $\{E_{t,i}^{\text{Ind},2} : t = 0, 1, \dots, T\}$. Keep this process until the difference between $\{E_{t,i}^{\text{Ind},j} : t = 0, 1, \dots, T\}$ and $\{E_{t,i}^{\text{Ind},j+1} : t = 0, 1, \dots, T\}$ is small for both i , that is,

$$\max_{t,i} \frac{|E_{t,i}^{\text{Ind},j+1} - E_{t,i}^{\text{Ind},j}|}{1 + |E_{t,i}^{\text{Ind},j}|} < \epsilon$$

In our case, we use $\epsilon = 10^{-6}$ as the stopping criterion.

A.3 Variables and Values of Parameters

In our model, we approximate the land carbon emissions E_t^{Land} and exogenous radiative forcing by the annual analogs of the corresponding paths of DICE-2016R (in five-year time steps) as follows:

$$E_t^{\text{Land}} = 0.95e^{-0.115t} \quad (\text{A.4})$$

$$F_t^{\text{EX}} = \begin{cases} 0.5 + 0.00588t, & \text{if } t \leq 85 \\ 1, & \text{otherwise} \end{cases} \quad (\text{A.5})$$

We follow Cai et al. (2019) to specify the abatement cost and the carbon intensity:

$$\theta_{1,t,i} = b_{0,i} \exp(-\alpha_i^b t) \sigma_{t,i} / \theta_2$$

$$\sigma_{t,i} = \sigma_{0,i} \exp(-\alpha_i^\sigma (1 - \exp(-d_i^\sigma t)) / d_i^\sigma)$$

Tables A.1 lists the values and/or definition of all parameters, variables, and symbols in the climate system.

Tables A.2 lists the values and/or definition of all parameters, variables, and symbols in the economic system.

Table A.1: Parameters, variables, and symbols in the climate system

t	time in years ($t = 0$ represents year 2015)
$i \in \{1, 2, 3\}$	region i (for the climate system: north $i = 1$, tropic $i = 2$, south $i = 3$; for the economic system: north $i = 1$, tropic/south $i = 2$)
M_t^{AT}	carbon concentration in the atmosphere (billion tons); $M_0^{\text{AT}} = 851$
M_t^{UO}	carbon concentration in upper ocean (billion tons); $M_0^{\text{UO}} = 460$
M_t^{DO}	carbon concentration in deep ocean (billion tons); $M_0^{\text{DO}} = 1740$
$\mathbf{M}_t = (M_t^{\text{AT}}, M_t^{\text{UO}}, M_t^{\text{DO}})^\top$	carbon concentration vector
$T_{t,i}^{\text{AT}}$	regional atmospheric temperature increase above pre-industrial level (Celsius); $T_{0,1}^{\text{AT}} = 1.29, T_{0,2}^{\text{AT}} = 0.91, T_{0,3}^{\text{AT}} = 0.79$
T_t^{OC}	average ocean temperature increase (Celsius); $T_0^{\text{OC}} = 0.1$
$(T_{t,1}^{\text{AT}}, T_{t,2}^{\text{AT}}, T_{t,3}^{\text{AT}}, T_t^{\text{OC}})$	temperature vector
F_t	global radiative forcing
F_t^{EX}	exogenous radiative forcing
$\eta = 3.68$	radiative forcing parameter
Φ_{M}	transition matrix of carbon cycle
Φ_{T}	transition matrix of temperature system
$\phi_{1,2} = 0.0597, \phi_{2,3} = 0.012$	parameters in transition matrix of carbon cycle
$(M_*^{\text{AT}}, M_*^{\text{UO}}, M_*^{\text{DO}})$ $= (588, 360, 1720)$	pre-industrial carbon concentration
$\xi_1 = 0.037, \xi_2 = 0.034$	parameters in transition matrix of temperature system
$\xi_3 = 0.0006, \xi_4 = 0.011$	
$\xi_5 = 0.061, \xi_6 = 0.04$	
$\xi_7 = 0.0088, \xi_{\text{ECS}} = 3.1$	

Table A.2: Parameters, variables, and symbols in the economic system

$Y_{t,i}$	gross output
$A_{t,i}$	total productivity factor (TFP); $A_{0,1} = 6.724, A_{0,2} = 2.054$
$\zeta_{1,1}^{\text{TFP}} = 0.0169, \zeta_{1,2}^{\text{TFP}} = 0.0122$ $\zeta_{1,3}^{\text{TFP}} = 0.0088, \zeta_{1,4}^{\text{TFP}} = 0.0036$ $\delta_1^{\text{TFP}} = 0.557$	parameters for TFP of the North in the baseline case
$\zeta_{2,1}^{\text{TFP}} = 0.0385, \zeta_{2,2}^{\text{TFP}} = 0.0197$ $\zeta_{2,3}^{\text{TFP}} = 0.0472, \zeta_{2,4}^{\text{TFP}} = 0.0741$ $\delta_2^{\text{TFP}} = 0.695$	parameters for TFP of the Tropic/South in the baseline case
$L_{t,i}$ $K_{t,i}$ $\alpha = 0.3$ $\Psi_{t,i}$ $\mu_{t,i}$	population (in billions) capital (in \$ trillions); $K_{0,1} = 100, K_{0,2} = 53$ output elasticity of capital mitigation expenditure emission control rate
$E_t, E_{t,i}^{\text{Ind}}, E_t^{\text{Land}}$	global emission; regional industrial emission; land emission
$\sigma_{t,i}$ $\alpha_1^\sigma = 0.0156, \alpha_2^\sigma = 0.0063$ $d_1^\sigma = 0.0181, d_2^\sigma = 0.000698$ $\theta_2 = 2.8, \theta_3 = 0.01$ $\theta_{1,t,i}$ $b_{0,1} = 1.32, b_{0,1} = 1.68$ $\alpha_1^b = \alpha_2^b = 0.005$ $\delta_K = 0.1$ $c_{t,i}$ $\gamma = 1.45$ u $\beta = 0.985$	carbon intensity; $\sigma_{0,1} = 0.119, \sigma_{0,2} = 0.132$ initial declining rate of carbon intensity change rate of declining rate of carbon intensity mitigation cost parameter adjusted cost for backstop initial backstop price declining rate of backstop price annual depreciation rate of capital per-capita consumption elasticity of marginal utility per-capita utility function discount factor